

Politecnico di Torino

Universidad Politécnica de Madrid



Master Course in Civil Engineering

Academic Year 2018/2019

Master Thesis:

The effect of recycled steel fibres on the deflection of reinforced concrete beams

Supervisors

A. P. Fantilli

A. Pérez Caldentey

Candidate

Benedetta Orfeo

Abstract

Nowadays everybody knows how much the environmental degradation represents a problem caused by the global warming due to greenhouse gasses. The global average temperature is closely connected to the carbon dioxide: if emissions and concentrations in the atmosphere of CO₂ increase, also the global average temperature does.

The increasing of CO₂ has characterized the entire XIX century and it is reaching higher and higher values. It is mainly due to fossil fuels and changes in the use of soils, but a great percentage, almost 6%, is also given by the production process of concrete which significantly contributes to the growth of greenhouse gases in the atmosphere.

In order to provide an effective solution, new construction technologies are developed and, in particular, the introduction of new materials into the concrete mixture that could allow the reduce of cement production.

The aim of this thesis is to contribute, in some small way, to a bigger European project focused into the study of Fibre Reinforced Concrete (FRC) and, more precisely, into the analysis of beams' deflection behaviour.

Based on experimental results, a model is carried out in order to demonstrate that the use of recycled steel fibres, obtained from End-of-Life tires, represents a great advantage in terms of mechanical characteristics of the material and, thanks to them, it is possible to realise elements with smaller cross-sections, reducing, consequently, the cement production.

Index

Abstract.....	2
Introduction.....	5
Concrete production.....	6
1 Fibre Reinforced Concrete.....	8
1.1 Recycled steel fibres	10
1.2 Standards.....	12
1.2.1 The Italian Standard.....	13
2 Experimental Survey.....	16
2.1 Preliminary tests.....	16
2.1.1 Tensile flexural test.....	17
2.1.2 Four-point bending tensile flexural test	19
2.1.3 Three-point bending tensile flexural test	22
2.2 Preliminary test results	24
2.2.1 Tensile flexural tests	29
2.3 Experimental campaign.....	30
3 The Model.....	36
3.1 Constitutive laws for FRC.....	37
3.1.1 fib Model Code 2010	42
3.1.2 Rilem.....	44
3.2 Definition of the constitutive law.....	45

3.2.1	Compression	45
3.2.2	Tension.....	47
3.3	Moment – Curvature	50
3.4	Computation of the Deflection.....	54
4	Results.....	56
4.1	Comparison between numerical and experimental results.....	60
4.2	Analysis of the results	60
5	Conclusions.....	69
6	Figure Index.....	71
7	Table index	75
8	Bibliografy.....	77
9	Annexes	80
9.1	Moment-Curvature diagrams	81
9.2	Comparison between numerical and experimental results.....	85

Introduction

The developed study deals with concrete beams reinforced with conventional rebars and Recycled Steel Fibres (RSF). The main objective is to analyse the deflection of these elements subjected to increasing loads in order to demonstrate that hybrid structures¹ are stiffer and more ductile than the conventional Reinforced Concrete (RC) ones and this produces a reduction of maximum mid-span deflection.

The attention is, in fact, focused in the reduction of CO₂ during the production process of concrete: in order to decrease the contribute of cement industry to climate change, it might be useful to realise more slender structures employing less material and FRC could represent the means to reach this purpose improving, on the one hand, the sustainability of RC structures using recycled materials and, on the other, enhancing their durability.

This strategy is effective in elements with low reinforcement ratios, which are typically slab-type structures, and it can be done if they are governed by serviceability conditions through the improvement of concrete contribution in tension.

RSFs are obtained by End-of-Life Tyres and, because of recycling process that is focused on the rubber rather than on the steel, they have variable length and they come out crooked. Nevertheless, their effectiveness and usability in concrete have been validated by Pérez, Groli et al. [2] and it has been possible to conduct an experimental campaign studying the Load-Deflection behaviour of eight beams varying RSF content, amount of tensile reinforcement and concrete cover.

The obtained results are, then, compared with a proposed model, built on the base of mechanical and geometrical properties of the elements object of study, together with the load values that they have to support. The matching among the empirical and numerical

¹ This is how elements reinforced with both rebars and steel fibres are called.

results allows to reach important satisfactory conclusions on the improvement on deflection behaviour due to the addition of RSF.

Concrete production

A little focus has to be done on the process of production of concrete in order to understand how, effectively, it contributes to the growth of greenhouse gases in the atmosphere.

Into the construction framework, concrete represents the most important material employed and it is used in a wide variety of products such as buildings, bridges, road, etc. Added to the ease of its production and to the great mechanical properties that characterize it, there is the advantage for which, at the end of the life cycle, concrete is often recycled and used again as a secondary constituent for other structures, i.e. streets for base course or as a filling material.

Concrete is a mixture of water, cement, aggregates and additives. In particular, the cement represents the binder and it is a finely ground inorganic material obtained by grading the cooking products of a mixture of clay, limestone and sand (obtained by clinker) with a small addition of gypsum and other elements such as natural pozzolana, micro-silica, fly ash and blast furnace slag. When the cement is mixed with water, creates a paste that sets thanks to reaction and hydration processes. Once hardened, it maintains its resistance and its stability even under water.

During the process to obtain cement, a fundamental step consists in the production and grinding of the clinker: it requires high temperatures and a large amount of energy. Nowadays, the contribution of this energy is still mainly given by fossil fuel derivatives such as oil and coal. This makes cement and, consequently, concrete responsible for 5.6% of carbon dioxide emissions and so the largest global industrial emitter. Moreover, an energy supply has to be added for packaging and transporting of the material, together with its use on site.

The effect of recycled steel fibres on the deflection of reinforced concrete beams

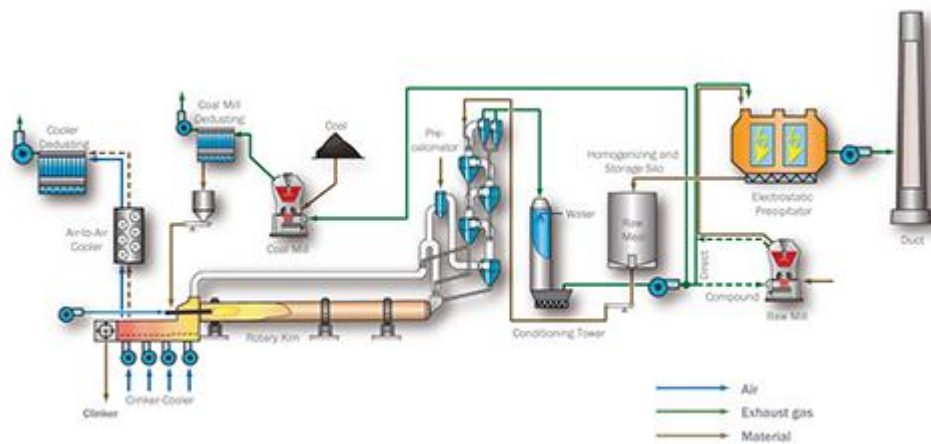


Figure 1 Production process of cement

“Blue Map Scenario” represents a project designed by the International Energy Agency (IEA) and born to co-operate with industries in order to draw up a reduction program for energy emissions. As far as cement and concrete industries concern, this reduction should reach 50% between 2006 and 2050. The goal is to develop energy security, to improve low-carbon technology and to bring benefits to people both economically and from a health perspective [1].

1 Fibre Reinforced Concrete

Fibre Reinforced Concrete (FRC) is a particular concrete containing fibrous material which increases its structural and mechanical characteristics with the aim of reducing its fragility and, above all, to be a bridge across the cracks that develop in concrete as it is stressed. The fibres are added during concrete production into the traditional cement matrix, characterized by water, cement, aggregates and additives, and they are scattered with uniform distribution and random orientation [3]. They include steel fibres, synthetic fibres, natural fibres and glass fibres.



Figure 2 Examples of fibres' materials

The behaviour of concrete changes with varying concrete, fibre material, geometries, orientation and densities.

Actually, this material is not as new as it is thought. Egyptians used to add straw to mudbricks or horsehair was used in mortar. In the 1900s, also asbestos was inserted in concrete, but in the 1950s, the health risks associated to asbestos were discovered and the need of finding a replacement fibre material born [4]. This is how steel, glass and

synthetic fibres were introduced and research in new fibre-reinforced concretes continues today.

Nowadays, many different fibre typologies are available and they differ for shape and dimensions.

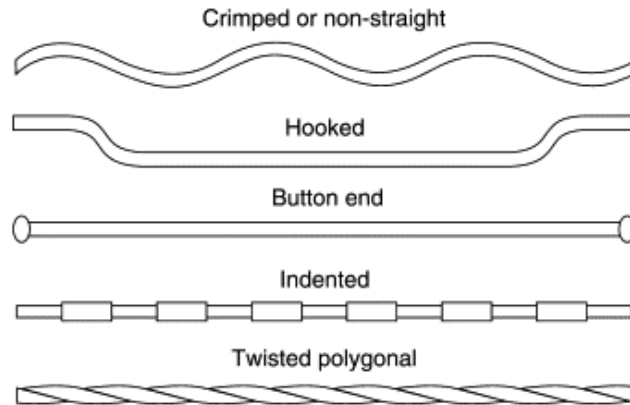


Figure 3. Some type of available steel fibres.

These geometries are developed in order to improve the mechanical anchorage, which is the most important of the bonding mechanisms. To improve fibre-matrix bond, surface treatments can be usually employed, such as in the case of synthetic fibres. Moreover, the mechanical behaviour of FRC depends also on physical and chemical adhesion and friction. In fact, at the fibre-matrix interface, shear stresses can develop because of the great difference between the fibres and the matrix elastic moduli. When this shear stress is exceeded, debonding gradually begins to occur and frictional shear stresses become the dominant stress transfer mechanism causing some cracking of the matrix [5].

The fibres are useful in providing greater resistance to plastic shrinkage cracking and service-related cracking. They have good resistance to impact, vibration, blasts and they are very useful in shotcrete and in thin overlays that are not sufficiently thick to accommodate reinforcing bars, although fibres are, generally, not intended as primary reinforcing.

Among all the properties of this material, some disadvantages compare: the reduced workability of the mixture due to the presence of fibres and the possibility of corrosion strains if the steel elements are exposed at the surface are two significant problems to face

with [6]. To easily solve the first problem, some superplasticizers additives or self-compacting concrete could be used.

On the other hand, it is important to underline that the fibres significantly confer and increase tensile strength to conventional concrete which, otherwise, gives its contribute only in compression. It means that once the deformation of the first crack is reached, FRC has an elastic-plastic behaviour, and so a ductile behaviour, in the post-cracked phase, i.e. it is able to withstand loads even after the onset of the first cracks.

1.1 Recycled steel fibres

According to the European Tyre Recycling Association (ETRA)², around 3 million tonnes Post-Consumer tyres are disposed of every year in the EU countries, roughly corresponding to 8 kg per person each year. This fact, added to the great intrinsic value of the tyre components (rubber, steel and textile), inspired European Directive 2008/98 that boosted tyre recycling all over Europe.

As pointed out by Centoze et al. [7], until thirty years ago, there were two ways for disposing of End-of-Life tyres: pile them up or landfill disposal, with their respective environmental implications.



Figure 4 Recycled rubber in various sizes

² See ETRA, *Introduction to tyre recycling*.

Generally, the recycling industry is focused on rubber revalorisation: it is normally granulated and used in several applications such as artificial lawn, asphalts, backfilling in civil works, etc.

Actually, the recycling process is usually obtained by mechanical treatments, microwave induced pyrolysis or breaking up of frozen tyres and it is based upon the separation of three components: the rubber, the steel and the textile. In fact, to provide tyres with strength and durability, they are reinforced with steel chords and textiles.

The steel chord invariably gets broken down to steel fibres when the tyre is crushed, independently from the recycling technology used, and the maximum length of fibres is fixed although the length distribution is stochastic. If this maximum length is too great, fibres come out balled together and cannot be placed directly into concrete.



Figure 5 Recycled steel fibres from End-of-Life tyres

As it is well known, bond properties are fundamental in determining FRC behaviour. This can be evaluated by the slenderness ratio, which is the length divided by the diameter. Since the diameter of recycled fibres is almost constant and around 0.3 mm, the length of the fibres determines their efficiency: longer fibres exhibit better post-crack behaviour as a consequence of the better bond conditions. On the other hand, if the maximum length is too high, fibres will ball together.

The scrap is usually sent to steel mills to obtain new steel; before it can be melted, it has to be processed to make it clean enough (< 5% of rubber) to be accepted by foundries. This added cost makes the price at which recovered steel is bought very small: depending on steel market fluctuation, it is about 140 €/ton.

Moreover, the process of steel re-melting is energy-consuming: it involves transport to a steel mill, melting and processing. If new steel fibres have to be obtained from it, extrusion, steel wire cutting and shaping are needed. By contrast, the only energy-consuming process needed to obtain fibres ready to use in concrete is fibre unballing by vibration and sieving.

When comparing the kgs of CO₂ emitted to obtain one ton of new steel fibres and to process one ton of recycled ones for direct use, environmental benefits are very remarkable, as shown in Figure 6.

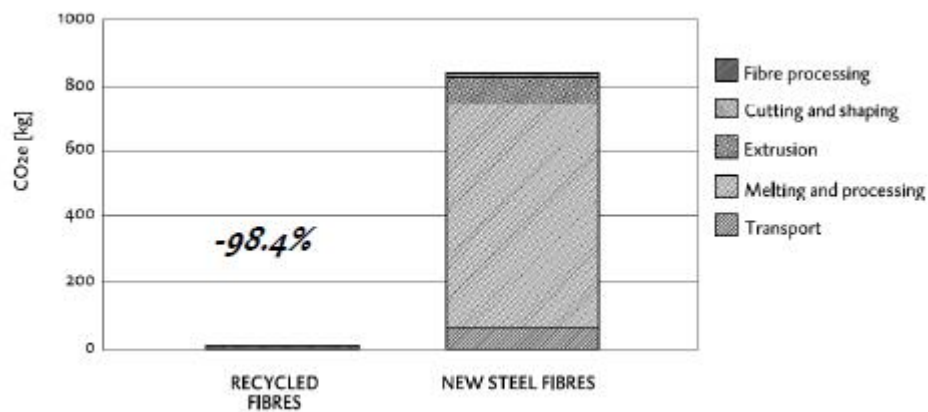


Figure 6 Comparison between emitted CO₂ kgs to obtain one ton of new steel fibres from scrap steel and process the recycled ones for direct use

On the other hand, new commercial fibres for concrete reinforcement cost around 900 €/ton. That is, once the recycled fibres are proven to be effective both for concreting and structural point of view, they have a great economic potential [8].

1.2 Standards

In the last three decades, many energies have been spent in the study of FRC mechanical properties, since it is considered one of the most relevant innovations in the field of special concretes. Nevertheless, the lack of international codes and guidelines for the design of FRC elements for many years hindered its expansion as a competitive structural solution.

Fortunately, throughout the last ten years, the publication of design codes and recommendations in Europe has represented a turning point to the incorporation of fibres as a reinforcing material. In order of appearance, some Standards: the German code [10], the RILEM Scientific Committee 162 recommendations [11], the Italian guideline [12], the European UNI EN 14651 [13], the Spanish code [14], the fib Model Code [15] and the Italian NTC [9].

Through the EHE-08 [14], it emerges that the Spanish code allows the partial or total substitution of rebars for structural fibres [17]. This idea has led to consider the structural contribution of fibres and the optimization of the amount of reinforcing rebars. Thanks to this, the prospective of employment of FRC has changed: FRC and RC-FRC³ have become a competitive design alternative both from the technical and the economic point of view and the use of fibres is no longer limited to improve durability by means of cracking control.

In order to design FRC structures it is essential to have solid, rational and reliable models to reproduce the behaviour of FRC as indicated in [16].

1.2.1 The Italian Standard

A little focus is done on the Italian Recommendation analysing how the application of fibre reinforced material has changed.

Within the Italian regulatory framework, all the products used into the structural process are described in the Chapter 11 of the NTC18 [9] and, in particular, the fibre reinforced concrete is mentioned into the paragraph 11.2.12, where it is underlined that it has to be CE⁴ marked according to the European standards, UNI EN 14889-1 and UNI EN 14889-2, and it shall be subject to a preliminary assessment according to the indications given in the §11.2.3 with the consequent definition of tensile strength values. In fact, what distinguishes FRC from ordinary concrete, is the presence of tensile strength which is

³ RC-FRC: combined solution of traditional reinforced concrete (RC) and FRC. Also called *hybrid structures*.

⁴ CE marking is a certification mark that indicates conformity with health, safety and environmental protection standards for products sold within the European Economic Area (EEA).

identified through two tensile residual strength parameters defined into UNI EN 14651:2007 [13]:

- Tensile serviceability residual strength, f_{R1k} ;
- Tensile ultimate residual strength, f_{R3k} .

With reference to CNR [12], the minimum amount of fibres to use in order to consider FRC as a structural material is 0.3% in volume and the design of the elements has to be done considering no presence of fibre to be on a safer side during the planning.

Finally, the recommendations for the production process of fibre reinforced concrete are defined into the Guidelines [18, 19].

The aforementioned considerations are related to the characteristics of the material, but as far as its employment into the structural framework concerns, it is necessary to make reference to NTC 2008 and NTC 2018 [9]. As briefly mentioned, there has been some changes from the old to the updated Reference Document.

As for NTC18, also into NTC08 it is considered necessary to differentiate “existing structures” from “structure to build”. Directly mentioning the Standard and, in particular, the paragraph 4.6 “Costruzioni di altri materiali”:

“I materiali non tradizionali o non trattati nelle presenti norme tecniche potranno essere utilizzati per la realizzazione di elementi strutturali od opere, previa autorizzazione del Servizio Tecnico Centrale su parere del Consiglio Superiore dei Lavori Pubblici, autorizzazione che riguarderà l’utilizzo del materiale nelle specifiche tipologie strutturali proposte sulla base di procedure definite dal Servizio Tecnico Centrale. Si intende qui riferirsi a materiali quali calcestruzzi di classe di resistenza superiore a C70/85, calcestruzzi fibrorinforzati, etc...”

On the other hand, for “existing structures”, the paragraph 8.6 explains:

“Gli interventi sulle strutture esistenti devono essere effettuati con i materiali previsti dalle presenti norme; possono altresì essere utilizzati materiali non tradizionali, purché nel rispetto di normative e documenti di comprovata validità, ovvero quelli elencati al cap. 12”.

Into the Chapter 12, it is clarified that:

“...a integrazione delle presenti norme e per quanto con esse non in contrasto, possono essere utilizzati i documenti di seguito indicati che costituiscono riferimenti di comprovata validità: Istruzioni del Consiglio Superiore dei Lavori Pubblici; Linee Guida del Servizio Tecnico Centrale del Consiglio Superiore dei Lavori Pubblici; Linee Guida per la valutazione e riduzione del rischio sismico del patrimonio culturale e successive modificazioni del Ministero; Istruzioni e documenti tecnici del Consiglio Nazionale delle Ricerche (C.N.R.), previo parere del Consiglio Superiore dei Lavori [...] Per quanto non trattato nella presente norma o nei documenti di comprovata validità sopra elencati, possono essere utilizzati anche altri codici internazionali...”

Summarizing, with respect to the material mentioned into Chapter 12 of NTC 2008, the design of FRC structures is allowed. On the contrary, to intervene on built constructions, an authorization is necessary.

NTC 2018 contains the same guidelines when it is referred to existing structures. Instead, for new constructions, any reference to fibre reinforced concrete has been deleted, but it has been clarified that structural materials or products used in the construction system shall be complies with the requirements of Chapter 11.

2 Experimental Survey

The developed studies have been started with the analysis of experimental results kindly provided by the professor Pérez. The aim is to observe the behaviour, in terms of deflection, of reinforced beams subjected to increasing loads and to realize a model in order to theorize and predict the deformation mechanisms of FRC elements. All the tests were carried out at the Structures Laboratory of the Civil Engineering School of the Polytechnic University of Madrid by Pérez et al.

2.1 Preliminary tests

As for ordinary concrete, also for FRC it is necessary to characterize the material carrying out compression tests to define the class, the strengths and the elastic modulus. Actually, the probably most relevant advantage of using steel fibres into concrete mixture is their capability to confer tensile strength to traditional concrete, which is possible to observe in the post-peak behaviour. In order to evaluate this important aspect, which is not possible to generalize because of the great variety of fibres' dimensions and materials available on the global market, also tensile flexural tests have to be done.

The direct tensile test is not usually performed because it is not easy to carry out and, above all, it is almost impossible to outline the post-cracking phase. Moreover, this test is not standardized and it is still subject of research.

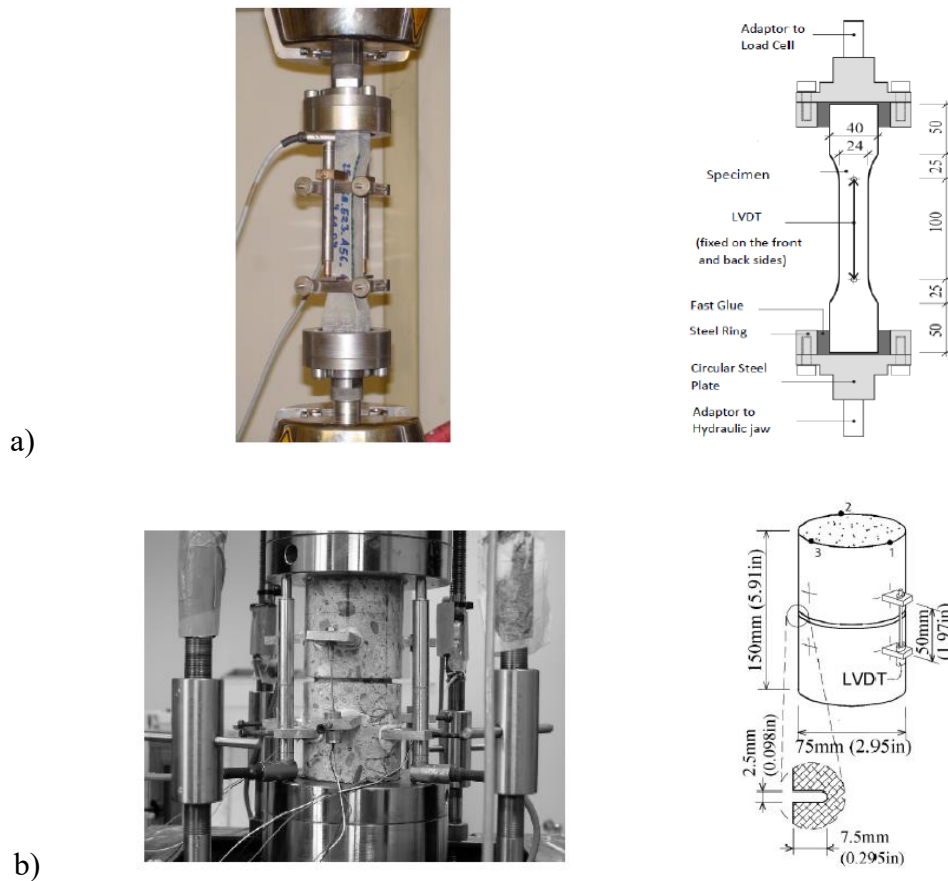


Figure 7 Direct tensile test on a) bone and b) cylinder specimens

Tensile flexural tests shall be carried out to address problems related to the direct tensile tests.

2.1.1 Tensile flexural test

The most common test for FRC characterization is the tensile flexural test performed on prismatic specimens. Depending on the Reference Standard, it can be performed on samples of different sizes with three or four point loads and with or without a midspan notch that enables the localization of the crack and, therefore, its opening (COD, *Crack Opening Displacement*) as a control parameter of the test. The three-point bending test is mostly used in Europe and it follows the lines described into the EN 14651 Standard [13]. On the other hand, the American ASTM C1609/1609M [20] defines the four-point bending test, especially carried out in America and in Japan [4].

The results in output from the test are the $\sigma-w$ graph in the case of notched specimen and the $\sigma-\varepsilon$ diagram for samples without the midspan notch, where σ is the stress applied, w is the crack width and ε is the strain of the element due to the load.

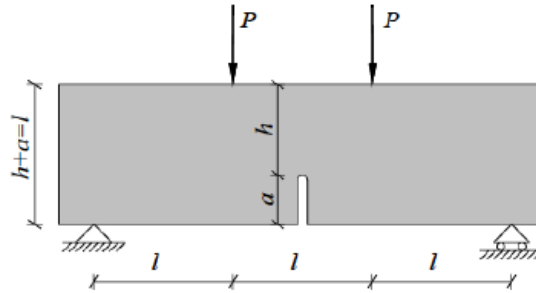


Figure 8 Notched specimen

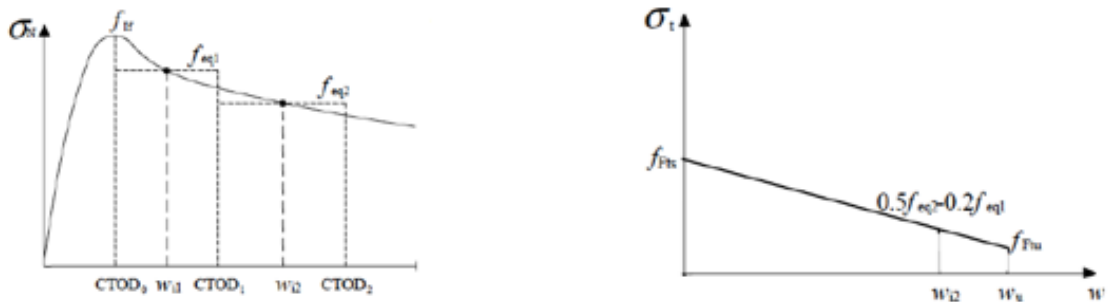


Figure 9 Attended results for notched specimens

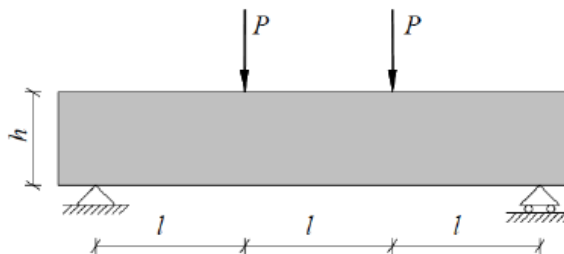


Figure 10 Non-notched specimen

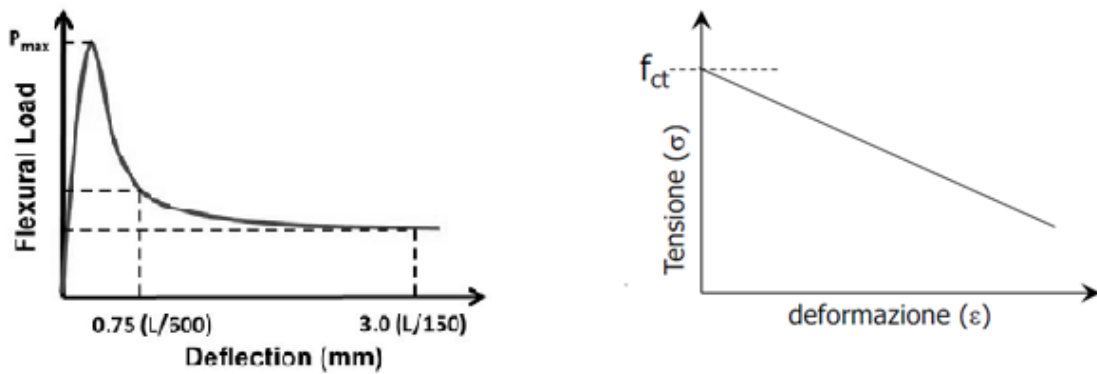


Figure 11 Attended results for specimens without notch

The reason of the diffusion of the tensile flexural test resides in the simplicity of performing it and in the reliability of the results. Moreover, the most recent design codes allow previsions for the use of FRC and its characterization is based on tensile flexural test on 15x15x60 cm notched specimens as in EN 14651:2007 Standard [13].

2.1.2 Four-point bending tensile flexural test

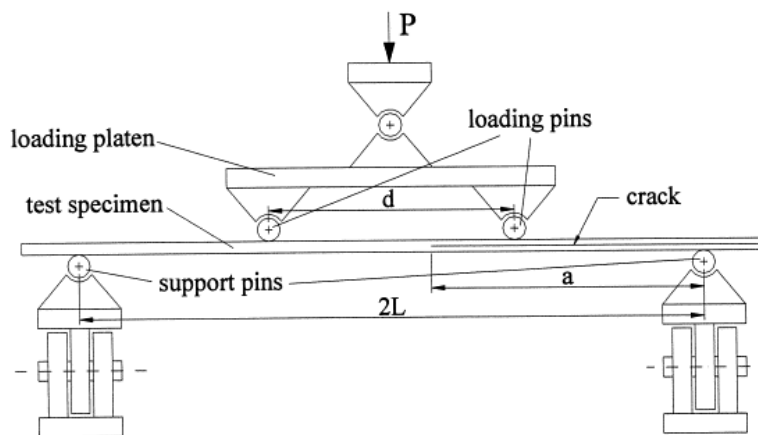


Figure 12 Tensile flexural specimen according to ASTM C1609/1609M

The American Standard ASTM C1609/1609M [20] suggests that the test has to be done with beams of dimensions 100x100x350 mm or of 150x150x500 mm in the case in which the length of the fibres is higher than 50 mm. The measurements are related to Load-Deflection and the test is stopped when the central arrow reaches a value of $L/150$.

The attended results could be represented in the following pictures:

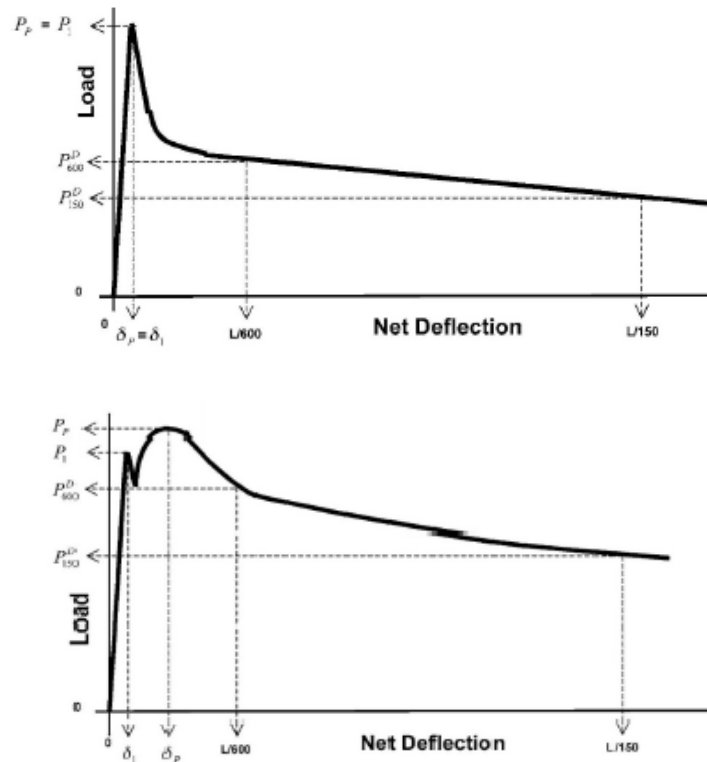


Figure 13 Attended results of 4-point bending tensile flexural test

P_1	first-peak load
P_p	peak load
δ_1	net deflection at first-peak load
δ_2	net deflection at peak load
f_1	first-peak strength
f_2	peak strength
P_{600}^D	residual load at net deflection of $L/600$
f_{600}^D	residual strength at net deflection of $L/600$
P_{150}^D	residual load at net deflection of $L/150$
f_{150}^D	residual strength at net deflection of $L/150$
T_{150}^D	area under the load vs. net deflection curve 0 to $L/150$

The answer of the beam to the applied load depends on the presence and on the amount of reinforcement that it contains. The optimum quantity in order to have an ideal behavior is $\rho_{min} \leq \rho \leq \rho_{max}$.

$$\rho = \frac{A_s}{A_c}$$

- ρ percentage of reinforcement
- ρ_{max} maximum percentage of reinforcement
- ρ_{min} minimum percentage of reinforcement
- A_s area of rebars in tension
- A_c area of rebars in compression
- η deflection
- P load
- A_i first crack
- B_i yielding

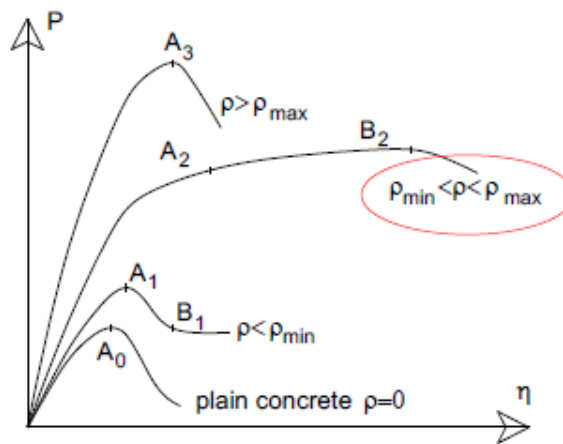


Figure 14 Possible P - η behaviour depending on reinforcement

The parameter evaluated through the test is then the residual strength:

$$f = \frac{2PL}{BH^2}$$

- L span length
- P load

The test is carried out by controlling the CMOD (Crack Mouth Opening Displacement) with a velocity of 0.05 mm/min if $CMOD \leq 0.1$ mm and of 0.2 mm/min when $CMOD > 0.1$ mm.

The objective is to evaluate the characteristic parameters defined in the following Figure:

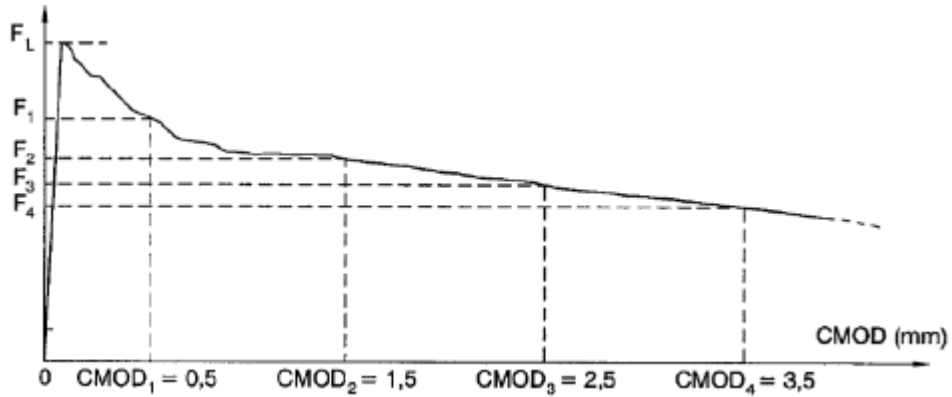


Figure 17 Typical Load-CMOD diagram

f_L = flexural strength \rightarrow corresponding to F-CMOD peak

$$f_{R,1} \rightarrow CMOD_1 = 0.5 \text{ mm} \quad \delta_{R,1} = 0.46 \text{ mm}$$

$$f_{R,2} \rightarrow CMOD_2 = 1.5 \text{ mm} \quad \delta_{R,1} = 1.31 \text{ mm}$$

$$f_{R,3} \rightarrow CMOD_3 = 2.5 \text{ mm} \quad \delta_{R,1} = 2.16 \text{ mm}$$

$$f_{R,4} \rightarrow CMOD_4 = 3.5 \text{ mm} \quad \delta_{R,1} = 3.00 \text{ mm}$$

with δ : mid-span deflection

Then, residual stresses are defined based on Navier-Bernoulli assumptions, i.e. considering a linear, non-cracked analysis within the section above the notch:

$$f_{R,j} = \frac{3F_j l}{2bh_{sp}^2}$$

$f_{R,j}$ residual strength for $CMOD=CMOD_j$

F_j force for $CMOD=CMOD_j$

l span

b specimen width

h_{sp} distance between the top of the notch and the top of the specimen

This test also allows midspan deflection's measurements through the following relation:

$$CMOD = 0.85 \delta + 0.04 \quad (in \text{ mm}).$$

It is worthy to point out that residual strengths do not represent actual stress levels in the material, since the Navier-Bernoulli assumptions is very unlikely to be met [2]. They are rather standardized indicators of the post-peak characteristics of the materials and, for this reason, minimum requirements for residual strengths are set in EHE-08 [14] and MC2010 [15] for an FRC to be considered suitable for structural use:

$$f_{R1k} \geq 0.4 f_{Lk}$$

$$f_{R3k} \geq 0.5 f_{R1k}.$$

2.2 Preliminary test results

First of all, it is necessary to take a step back and make some considerations on the choice of the material used for casting FRC specimens. The following considerations are related to a previous analysis conducted by Pérez, Groli et al., deeply described into Groli's PhD thesis [2].

The elements are characterized by conventional concrete $f_{ck}=25$ MPa with coarse aggregate, whose diameter was limited to 12 mm to avoid balling.

Table 1 Composition of concrete per m^3 for preliminary tests

CEM II 42.5 R	310 kg
Water	150 l
0/6 mm aggregates	1018 kg
6/12 mm aggregates	825 kg
Superplasticizer	2.6 l
W/C	0.48
C/ aggregates	0.17

In order to identify the typology of fibers needed, Groli et al. [2] have conducted studies on several batches distinguished for different fiber type (commercial or recycled) and fiber content (from 0.5% to 1.3% in volume):

- Series TR – recycled short, $\frac{l}{\phi} \approx 50$;
- Series R – recycled long, $\frac{l}{\phi} \approx 150$;
- Series CH – commercial hooked, $\frac{l}{\phi} = 86$;
- Series C – commercial straight, $\frac{l}{\phi} = 81$.
-

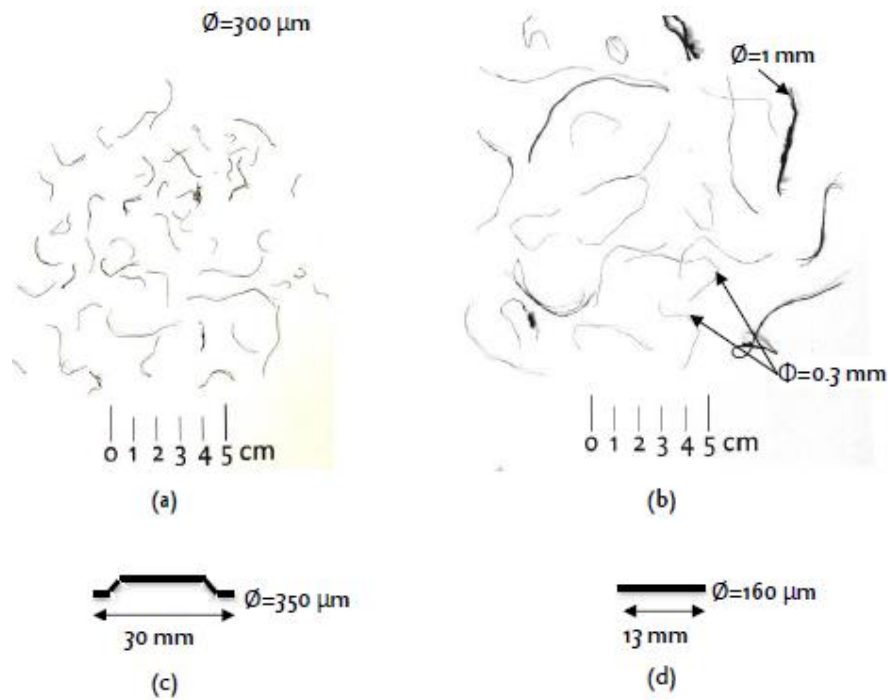


Figure 18 Fibres used in preliminary study: a) recycled short, series TR; b) recycled long, series R; c) commercial hooked, series CH; d) commercial straight, series C [2]

The characteristic strengths of batches are shown in Table 2, also counting the series H-0% that is the control batch of plain concrete.

Table 2 Summary of batches and characteristic strength taken by preliminary tests

Batch	Fiber content (V_f/V_c)	f_{cm}^* [MPa]	f_{ctm}^{**} [MPa]
H-0%	-	33.1	3.1
R-0.5%	0.50%	34.7	5.5
R-0.86%	0.86%	48.1	6.4
C-0.86%	0.86%	32.7	5.5
C-1.3%	1.30%	25.4	4.6
CH-0.7%	0.70%	39.0	4.7
TR-0.86%	0.86%	43.1	6.2
TR-1.2%	1.20%	39.3	6.1

*Cylinder compression test of FRC
 **Tensile indirect test con cylinders

The batch R showed some balling problems due to the length of the fibres. In fact, recycled fibres with aspect ratio $\frac{l}{\phi}$ around 200 lead to this problem.

Another consideration has to be done related to the fibre volume content: C and TR series have lost strength at high fibre dosage, in agreement with the results of Angelakopoulos et al. [21].

In order to characterize the material, two notched prismatic specimens for each batch were tested in 3-point flexural tensile tests by Pérez, Groli et al. [2]

Because of the geometry of the press available, the dimensions of the samples could not respect the requirements according to EN 14651, so notched prisms of 100x100x400 mm were used, although the test was carried out following the guidelines of the mentioned Standard in every other aspect.

The test is performed in displacement control of the CMOD (Crack Mouth Opening Displacement) and the results obtained are shown in Table 3 and in Figure 19.

Table 3 Tensile residual strengths of FRCs in preliminary tests [2]

Tensile residual strengths [MPa]				
	LOP	f_{R1m}	f_{R2m}	f_{R3m}
R-0.5%	5.6	5.6	5.6	4.2
R-0.86%	8.3	8.3	7.6	6.7
C-0.86%	5.8	3.6	2.8	2
C-1.3%	4.6	2.9	2.2	1.7
CH-0.7%	6.5	6.2	7.2	6.9
TR-0.86%	6	4.6	3.6	2.8
TR-1.2%	5.2	4.1	3.1	2.5

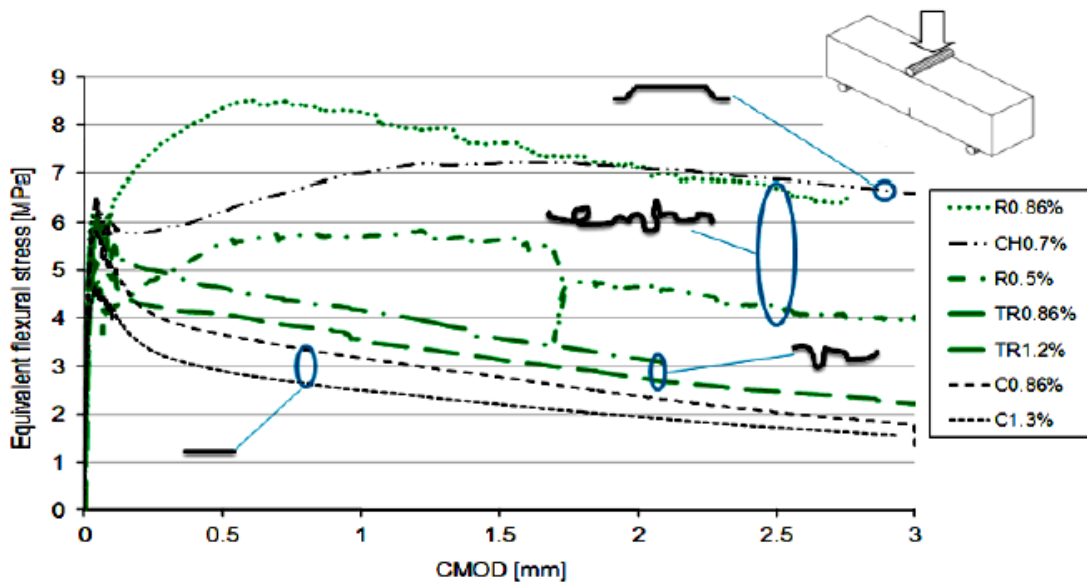


Figure 19 Comparison of 3-point tensile flexural tests. Green curves are for recycled fibres, while black ones are for commercial steel fibres [2]

From the results obtained, Groli has concluded that:

- As expected, fibres with better bond properties have better post-peak behaviour, such as R and CH series thanks to the hooks for commercial fibres and the greater length for recycled ones;
- On the contrary, shorter steel elements show a post-peak softening (C and TR series). It is also possible to see that C-1.3% and TR-1.2% are characterized by a

smaller peak than C-0.86% and TR-0.86%. This reflects the fact that there is an optimum fibre content after which FRC behaviour does not improve and, together with this, can even worsen due to the matrix weakening induced by poor concreting conditions.

The general good results shown by TR series in the previously showed tests, together with its relative ease in mixing and other considerations outlined by a more extensive experimental campaign carried out by Groli et al. [2], allowed to select screened recycled fibres as the most suitable to use.

Once the fibers are defined, Self-Compacting Concrete (SCC)⁵ was chosen for the campaign batches with a compressive strength of $f_{ck,28}=30$ MPa.

This decision is another consequence of the previous results for which the more fluid the concrete, the easier the mix. With the aim of characterize the mechanical properties of the material, compressive and indirect tensile tests were carried out at 7 and 28 days.

Table 4 Results for cylinder compression and indirect tension tests for SCC

	Cylinder compression f_{cm} [MPa]		Indirect tensile f_{ctm} [MPa]	
	7 days	28 days	7 days	28 days
0%	32.3	37.5	3.3	4.2
0.5%	33.4	36.4	2.7	3.1
1.0%	31.3	37.5	2.6	3.3

Fibre addition even at high dosage (1.0%) did not have a significant effect on compressive strength.

⁵ From other Groli's preliminary tests results [2], the more fluid the concrete, the easier the mix. So, for testing reasons, SCC was chosen.

2.2.1 Tensile flexural tests

Notched prisms of dimensions 15x15x60 cm and fibres content of 0.5% or 1.0% have been prepared, according to EN 14561 [13], and they have been subjected to tensile flexural tests. The results are shown in Figure 20 and Figure 21.

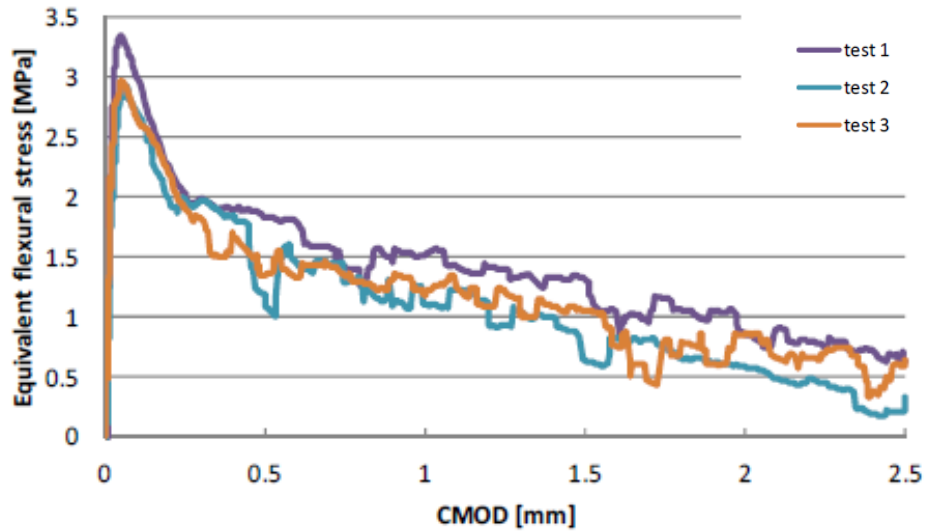


Figure 20 Results of tensile flexural test for specimens with 0.5% in volume of fibre

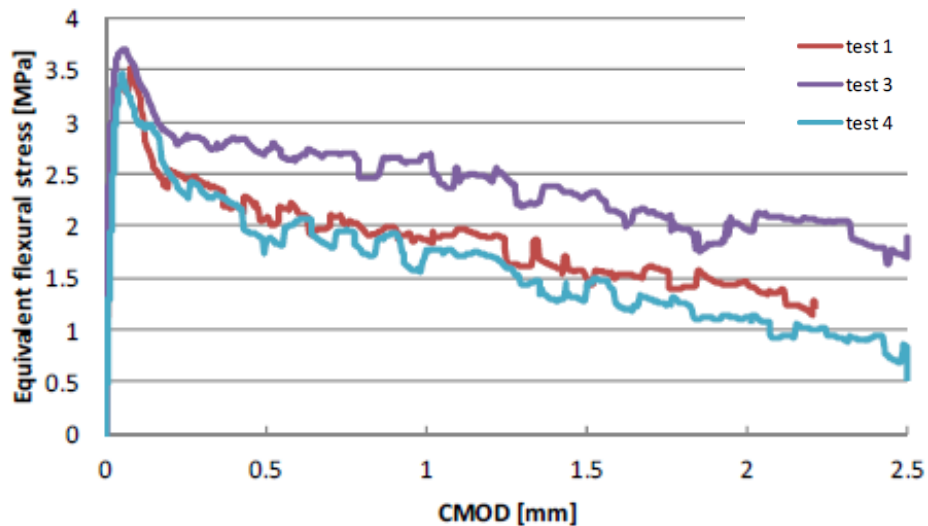


Figure 21 Results of tensile flexural test for specimens with 1.0% in volume of fibre

The values of tensile residual strengths measured are presented in Table 5.

Table 5 Tensile residual strengths according to EN 14651

Tensile residual strengths [MPa]				
	LOP	f_{R1m}	f_{R2m}	f_{R3m}
0.5%	3.10	1.53	1.08	0.51
1.0%	3.53	2.21	1.72	1.26

In accordance to MC2010 [15], the minimum requirements for residual strengths are checked in the Table 6.

Table 6 Minimum requirement according to MC2010

Check	f_{R1}	\geq	$0.4 f_L$
0.5%	1.53	\geq	1.24
1.0%	2.21	\geq	1.412
Check	f_{R3}	\geq	$0.5 f_{R1}$
0.5%	0.51	\geq	0.765
1.0%	1.26	\geq	1.105

It should be noted that 0.5% batch does not fulfil the requirement for FRC to be used as total or partial replacement of conventional reinforcement at ULS. However, it can be considered effective in terms of serviceability conditions, because the assessment $f_{R1m}/f_L \geq 0.4$ can be regarded as a “serviceability requirement”, so it results to be acceptable for the purpose of this thesis.

2.3 Experimental campaign

Once the preliminary tests have been done, four-point flexural bending tests on FRC beams are carried out by Pérez et al. with the goal of analyse their deflection due to increasing loads applied in the cantilever edges, that is the main objective of this thesis.

The experimental program involves eight beam specimens and, in order to take advantage of the results already obtained by Pérez et al. [24] for standard RC and therefore to enable

a clear comparison, the test set-up and specimen design was taken the same as in the above mentioned study, as shown in Figure 22 and Figure 23.



Figure 22 Cross-sections of the analysed beams (dimensions in mm); ZZ is the fibre content: 0%, 0.5% or 1.0%

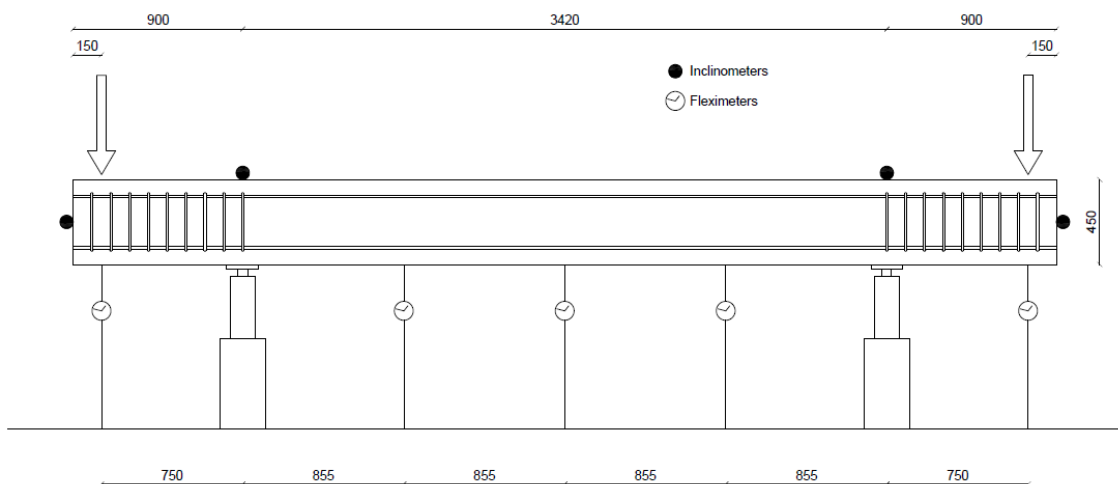


Figure 23 Four-point flexural bending test set-up

The tests feature point loading with a constant moment span of 3.42 m and they are performed on beams with rectangular cross section 0.35 m wide and 0.45 m in height. The type of concrete used for the casting is SCC 30/37 and the steel for reinforcement rebars is B-500-SD. All beams are reinforced in shear only in the cantilever region at the loading zones to prevent shear failure, but not in the central constant bending zone. Compressive reinforcement is always of diameter $\varnothing 12$.

The key parameters for which the beams are distinguished are:

- rebar diameters: 12 and 25 mm;
- concrete cover: 20 and 70 mm;
- fibres contents: 0% (plain concrete), 0.5% and 1.0%.

The elements are named with a code as XX-YY-ZZ where:

- XX is the diameter in mm of rebars in tension;
- YY is the concrete cover in mm;
- ZZ is the fibre content in percentage.

For the beams coded in the previous study [24], characterized by the presence of no fibres, the last two digits of the beam code refer to stirrup spacing: XX-YY-00 are the beams with no stirrups, XX-YY-10 and XX-YY-30 are the ones with stirrups distant from each other of, respectively, 10 and 30 cm.

All beams are loaded until failure, so that the serviceability working area could be fully explored. The recorded results are plotted in Figure 24, Figure 25, Figure 26 and Figure 27.

The effect of recycled steel fibres on the deflection of reinforced concrete beams

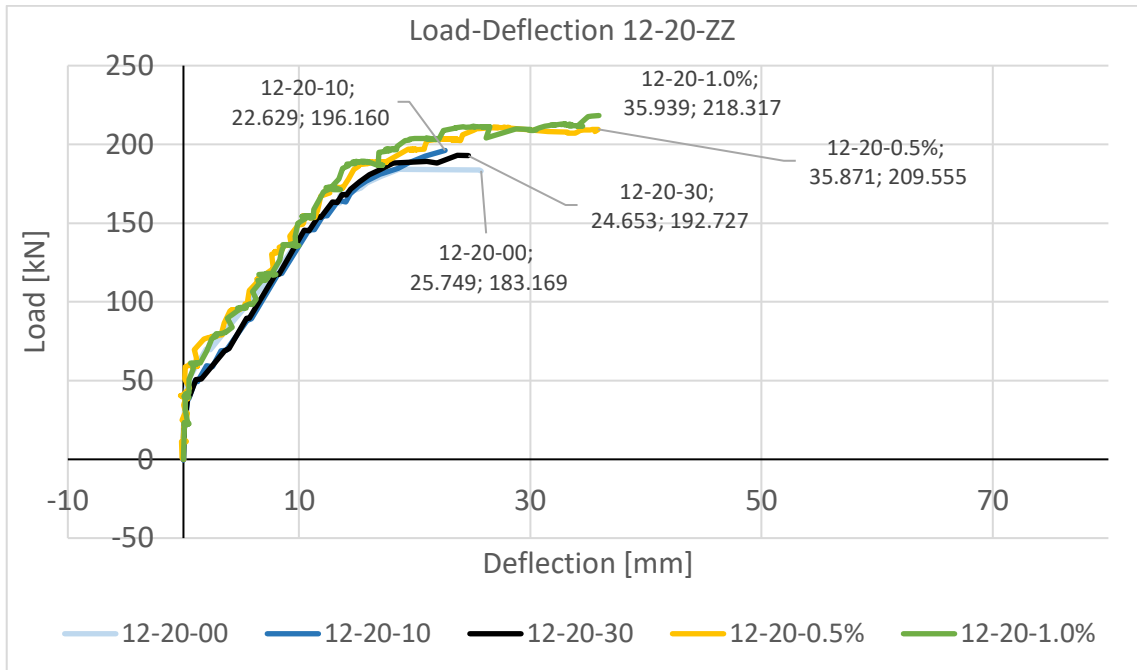


Figure 24 Load-deflection for 12-20-ZZ beams

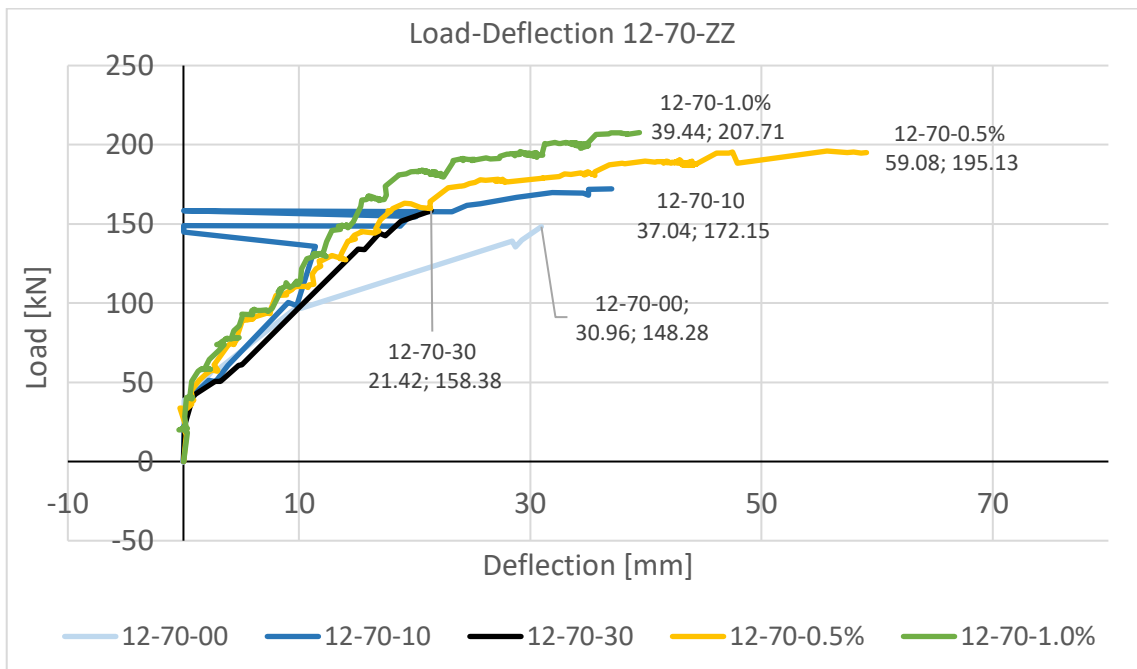


Figure 25 Load-deflection for 12-70-ZZ beams

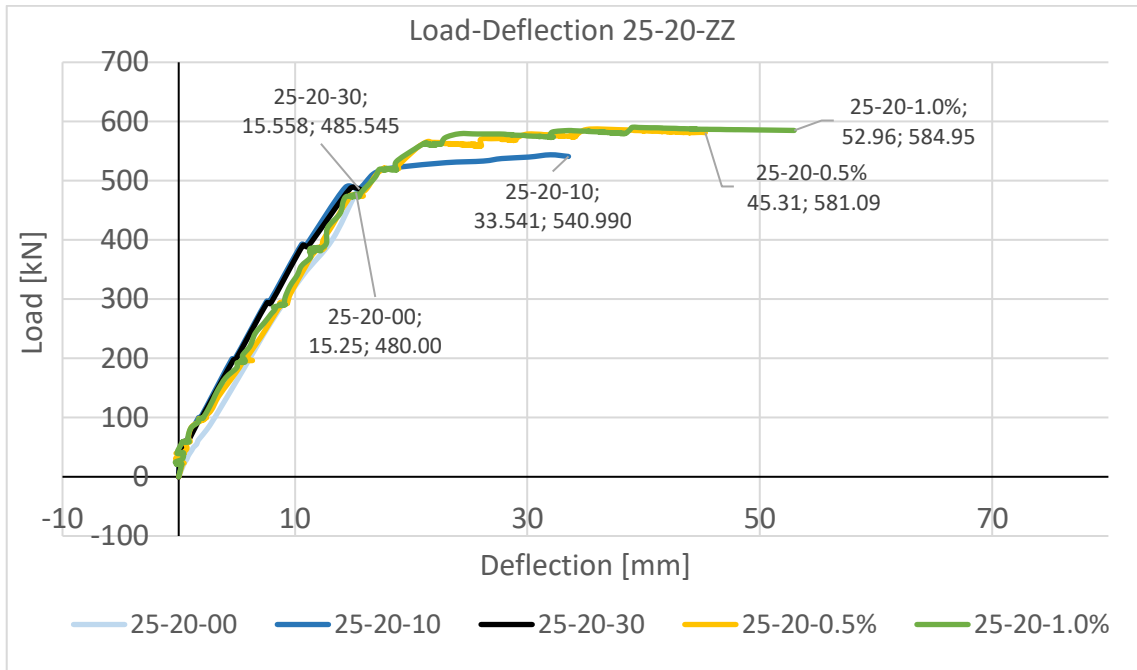


Figure 26 Load-deflection for 25-20-ZZ beams

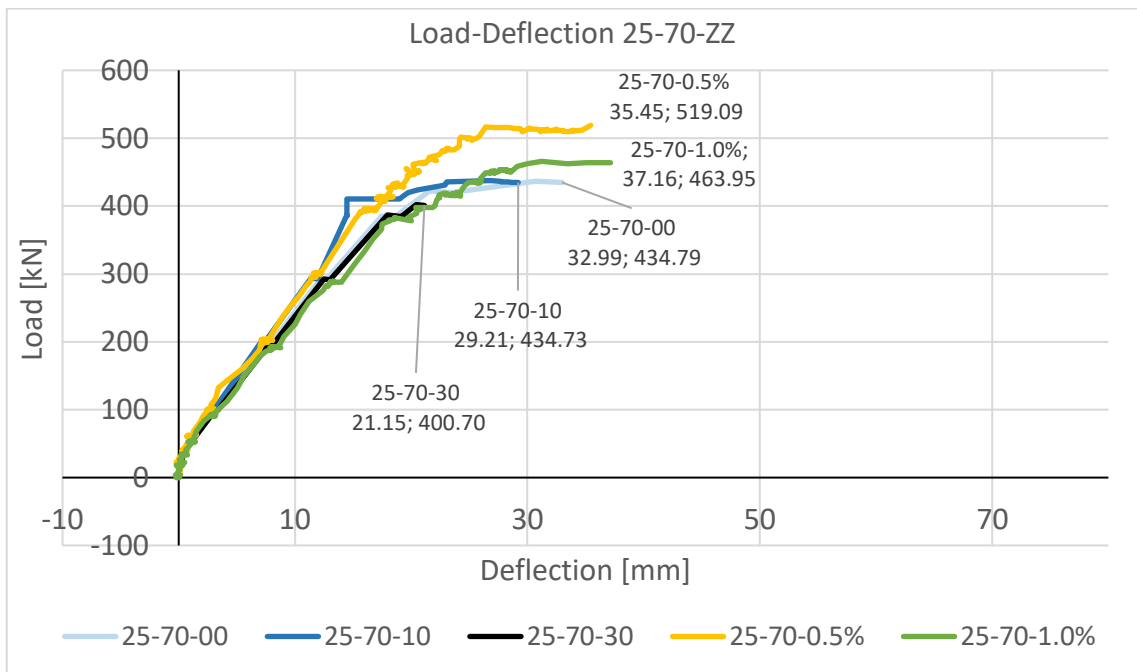


Figure 27 Load-deflection for 25-70-ZZ beams

Table 7 Estimated ultimate load values

Ultimate Load [kN]			
12-20-00	184	12-70-00	148
12-20-10	196	12-70-10	172
12-20-30	193	12-70-30	158
12-20-0.5%	210	12-70-0.5%	195
12-20-1.0%	218	12-70-1.0%	207
25-20-00	480	25-70-00	435
25-20-10	541	25-70-10	435
25-20-30	485.5	25-70-30	401
25-20-0.5%	587	25-70-0.5%	519
25-20-1.0%	590	25-70-1.0%	464

As one might suppose, the most evident results is that beams with higher diameter rebars are able to support higher loads. In fact, its order of magnitude for $\varnothing 12$ is around 150-200 kN against the 400-600 kN of 25 \varnothing rebars.

On the contrary, lower the concrete cover, higher the load and, as far as the amount of fibres concerns, more volume of fibre into the concrete mixture means higher loads, although at ULS it does not always occur.

3 The Model

The objective of creating a numerical model is to predict and theorize the behaviour of beams' deflection under the application of loads. What it is tried to achieve is a tool that allows good interpretation of experimental results to better underline the advantages of FRC beams.

The idea is to demonstrate that steel fibres could improve the performance of conventional concrete and then to contribute to its sustainability allowing the production of more slender elements thanks to the use of a recycled material.

The results obtained during the preliminary tests represent the base from which the model has been built: the first step has consisted in defining the constitutive law, determined knowing compressive and tensile strengths which have been respectively obtained through compressive and three-point flexural bending tests, to which the Rilem formulations are then applied. These values, together with the geometrical properties and the amount of reinforcement that characterise the beam, have allowed to define the Moment-Curvature diagrams, necessary for the functioning of the proposed model. To this, in fact, it has followed the computation of the final attended Load-Deflection values and the consequent respective trends, which have been compared to the ones obtained in the laboratory (see from Figure 24 to Figure 27).

3.1 Constitutive laws for FRC

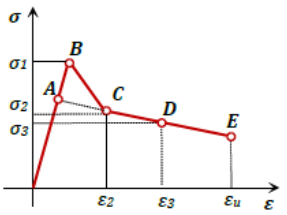
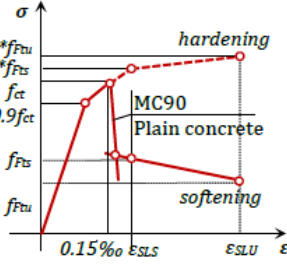
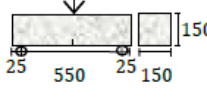
It is widely accepted that the addition of steel fibres in normal contents does not substantially affect the pre-cracking behaviour of FRC. This implies that compressive and pre-cracking elastic branches, basically E_c and f_{ct} , can be taken as the same for conventional concrete [2].

Over the past ten years, several technical guidelines have been published with the aim of facilitating the design of FRC structures defining its tensile behaviour. There is a number of models to describe it, although a basic distinction is made between the *smearred crack* and the *localized crack* models, which are respectively based on fracture mechanisms and so on the energy absorption properties, and on the resistance of materials. Most of these constitutive models are based on an indirect approach, requiring parameters that must be defined each time from experimental data. Less common are the models based on a direct approach that provides the same curves using basic properties of its constituent materials [22].

The identification of the most suitable constitutive model to simulate the tensile post-cracking behaviour represents one of the key steps in the design of FRC structures. In the Table 8, the constitutive models proposed by European standards are shown [9-15] grouped according to the type of diagram (rectangular, bilinear and trilinear or multilinear). The main parameters that define each one of the models are summarized, together with the schemes of the tests required to obtain the values of these parameters [22].

Table 8 Constitutive models in European guidelines [22]

Diagram	Parameters	Characterization Test	
	$\sigma_1 = f_{eq,ctd,II} = f_{eq,ctk,II} \cdot \alpha_c^f \cdot \alpha_{sys} / \gamma_{ct}^f \leq f_{eq,ctd,I}$ <p>(α_{sys}: coefficient for size effect; α_c^f: coefficient for longterm strength behaviour) $\epsilon_1 = \epsilon_u = 10\text{‰}$</p>	<p>DIN 1048</p>	DBV [10]
	$\sigma_1 = f_{Ftu} = f_{eq2}/3$ <p>$\epsilon_1 = \epsilon_u = [20\text{‰ softening} ; 10\text{‰ hardening}]$</p>	<p>UNI 11039</p>	CNR-DT 204 [12]
	$\sigma_1 = f_{ctRd} = 0.33 f_{R3,d}$ <p>$\epsilon_1 = \epsilon_u = [20\text{‰ bending} ; 10\text{‰ tensile}]$</p>	<p>UNE EN 14651</p>	EHE [14]
	$\sigma_1 = f_{Ftu} = f_{R3}/3$ <p>$\epsilon_1 = \epsilon_u = [20\text{‰ softening} ; 10\text{‰ hardening}]$</p>	<p>UNE EN 14651</p>	MC [15]
	$\sigma_1 = f_{eq,ctd,I} = f_{eq,ctk,I} \cdot \alpha_c^f \cdot \alpha_{sys} / \gamma_{ct}^f$ $\sigma_2 = f_{eq,ctd,II} = f_{eq,ctk,II} \cdot \alpha_c^f \cdot \alpha_{sys} / \gamma_{ct}^f \leq f_{eq,ctd,I}$ <p>$\epsilon_2 = \epsilon_u = 10\text{‰}$</p>	<p>DIN 1048</p>	DBV [10]
	$\sigma_1 = f_{Fts} = 0.45 f_{eq1}$ $\sigma_2 = f_{Ftu} = k [f_{Fts} - (w_u/w_{i2}) (f_{Fts} - 0.5 f_{eq2} + 0.2 f_{eq1})]$ <p>$k = [0.7 \text{ pure tension, } 1 \text{ other cases}]$ $\epsilon_2 = \epsilon_u = [20\text{‰ softening} ; 10\text{‰ hardening}]$</p>	<p>UNI 11039</p>	CNR-DT 204 [12]
	$\sigma_1 = f_{ctd} = \alpha_c^f \cdot f_{ctk,fl} / \gamma_{ct}^f$ $\sigma_2 = f_{eq,ctd,I} = f_{eq,ctk,I} \cdot \alpha_c^f \cdot \alpha_{sys} / \gamma_{ct}^f$ $\sigma_3 = f_{eq,ctd,II} = f_{eq,ctk,II} \cdot \alpha_c^f \cdot \alpha_{sys} / \gamma_{ct}^f \leq f_{eq,ctd,I}$ <p>$\epsilon_1 = \sigma_1 / E_{HRF}$; $\epsilon_2 = \epsilon_1 + 0.1\text{‰}$; $\epsilon_3 = \epsilon_u = 10\text{‰}$</p>	<p>DIN 1048</p>	DBV [10]
	$\sigma_1 = 0.7 f_{ctm,fl} (1.6 - d);$ $\sigma_2 = 0.45 \cdot \kappa_h \cdot f_{R,1};$ $\sigma_3 = 0.37 \cdot \kappa_h \cdot f_{R,4}$ <p>$\epsilon_1 = \sigma_1 / E_{HRF}$; $\epsilon_2 = \epsilon_1 + 0.1\text{‰}$; $\epsilon_3 = \epsilon_u = 25\text{‰}$</p>	<p>RILEM TEST</p>	RILEM [11]

	$\sigma_1 = f_{ct,d} = 0.6 f_{ct,f,d}$ $\sigma_2 = f_{ctR1,d} = 0.45 f_{R1,d}$ $\sigma_3 = f_{ctR3,d} = k_1 (0.5 f_{R3,d} - 0.2 f_{R1,d})$ $\varepsilon_2 = 0.1 + 1000 \cdot f_{ct,d} / E_{c,0}$ $\varepsilon_3 = 2.5 / l_{cs} \text{ (} l_{cs} \text{: characteristic length)}$ $\varepsilon_u = [20\% \text{ bending; } 10\% \text{ pure tension}]$	<p>UNE EN 14651</p> 	<p>EHE [14]</p>
	$f_{ctm} = f_{ctk0,m} (f_{ck}/f_{ck0})^{2/3}$ $f_{Fts} = 0.45 f_{R1}$ $f_{Ftu} = k [f_{Fts} - (w_u / CMOD_3) (f_{Fts} - 0.5 f_{R3} + 0.2 f_{R1})]$ $\varepsilon_{SLU} = CMOD_1 / l_{cs}$ $\varepsilon_{SLU} = w_u / l_{cs} = \min(\varepsilon_{Fu}, 2.5 / l_{cs} = 2.5 / y)$ $\varepsilon_{Fu} = [20\% \text{ softening; } 10\% \text{ hardening}]$	<p>UNE EN 14651</p> 	<p>MC [15]</p>

Moreover, Table 9 presents the criteria considered in each of the constitutive models introduced in Table 8. The models are listed according to the chronological order of publication, starting with the DBV [10], RILEM [11], CNR-DT 204 [12], EHE-08 [123] and ending with the *fib* Model Code [15].

Table 9 Characteristics of the constitutive models from guidelines [22]

	DBV [10]	RILEM [11]	CNR-DT 204 [12]	EHE [14]	MODEL CODE [15]
Stress- strain (ε)/ Stress-crack width (w)	ε	ε	ε/w	ε	ε/w
Direct approach (DA) / Indirect approach (IA)	IA	IA	IA	IA	IA
Continuous equation (CE) / Discontinuous equation (DE)	DE	DE	DE	DE	DE
Considers residual strengths		•		•	•
Considers equivalent strengths	•		•		
Differentiates the ultimate strain (20‰; 10‰)			•	•	•
Conversion factors regarding the linear-elastic distribution of stresses	•	•		•	
Uses the characteristic length to obtain strain			•	•	•
Considers safety coefficients	•		•	•	•

Considers size effect	•	•			
Considers the effect of sustained loads	•				
Considers fiber content					
Uses the terminology “structural fiber			•	•	•
Considers the contribution of fibers in the crack spacing		•	•		•
Considers fiber orientation in the design					•

It is important to underline that DBV [10] and RILEM [11] are among the first design guidelines and, with respect to the newer ones, they only refer to steel fibres whereas the latter differentiate structural and non-structural fibres⁶. This terminology implies a significant change in the design of FRC since it extends the range of fibres that may be used with structural purposes. Also the size effect is a common concept in the early design guidelines. It takes into account the effect of the height on the bending behaviour of the cross section by penalizing the section with larger height [22].

Constitutive laws can be σ - ε or σ - w diagrams, where w is the crack width opening, obtained in direct or indirect tension tests. The main advantage of using a σ - w model is that it can be directly compared to the experimental results, e.g. uniaxial tensile tests. With the σ - ε model the tensile and the compressive behaviours may be represented in a single diagram. Likewise, such approach is more convenient for practical reasons since it is the same used for traditional steel reinforcement.

⁶ Structural fibers are defined as those having a high modulus of elasticity and that, in a certain dosage, are able to guarantee minimum FRC performance in terms of toughness [23].

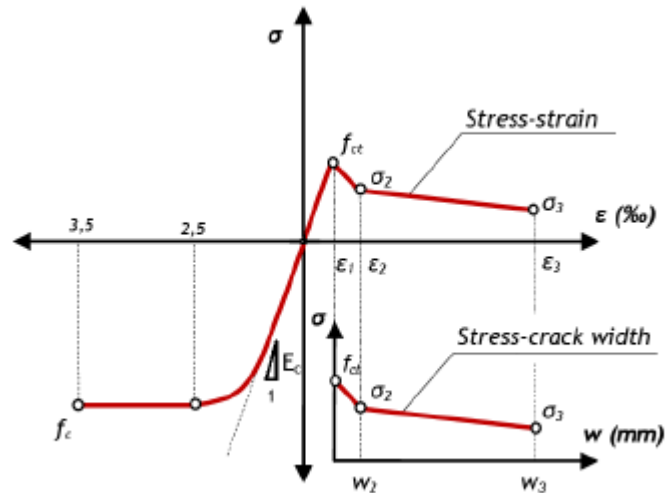


Figure 28 Stress-strain and stress- crack width models

There are several studies in the literature dedicated to the relation between the $\sigma-w$ diagram and the $\sigma-\varepsilon$ diagram. In fact, it is possible to normalize the x-axis of the $\sigma-w$ curve to $\sigma-\varepsilon$ dividing w by the structural characteristic length l_{cs} , according to the fact that the strain can be expressed as $\varepsilon=w/l_{cs}$. Model Code 2010 [15] defines the value of l_{cs} as the minimum between the average crack spacing s_m and the distance between the neutral axis and the most tensioned fibre of the cross-section, as shown in the following picture:

$$l_{cs} = \min(s_m, y)$$

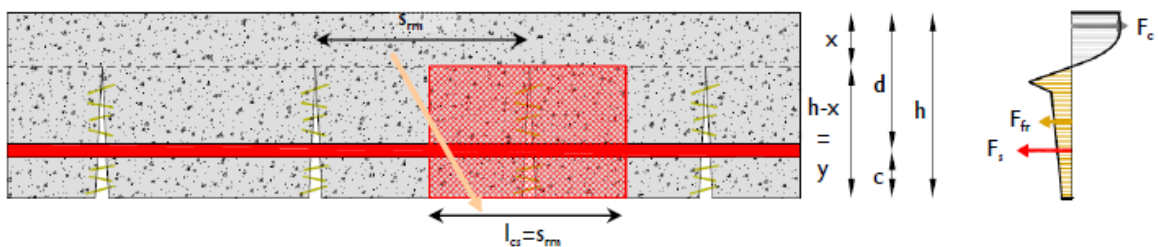


Figure 29 Structural characteristic length according to MC2010 [2]

In the case of elements with conventional reinforcement, y is evaluated in the cracked phase assuming no tensile strength of the FRC and a load configuration corresponding to the SLS of crack opening and crack spacing (see Figure 30a). In sections without traditional reinforcement under bending or under combined tensile-flexural and compressive-flexural forces with the resulting force external to the section, the value of y

is assumed equal to the height of the section (see Figure 30b). The use of the characteristic length is not necessary for hardening materials.

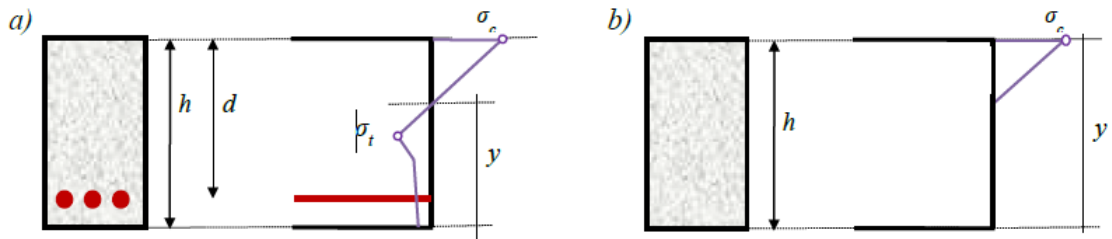


Figure 30 Definition of "y" for a) sections with traditional reinforcement and b) sections without traditional reinforcement [2]

As far as the characteristic length concerns, considering that the post-peak behaviour of FRC is governed by debonding of fibres, the assumption made by Fantilli et al. [16] of considering l_{cs} as the length of the fibre, should be taken.

Another problem is how to transform the residual tensile strength $f_{R,j}$ to effective stresses in the material. In order to do this, the focus is set on the two most used models: fib Model Code [15] and Rilem [11].

3.1.1 fib Model Code 2010

The fib⁷ Model Code 2010 represents an updated version of the CEB-FIP Model Code 90 and it is introduced with the aim of providing a tool for the design of FRC structural elements. It proposes two models for the tensile behaviour of FRC: the rigid-plastic and the linear-elastic behaviour, shown in the Figure 31. These models are presented in terms of simplified σ - w constitutive laws and reproduce materials with hardening and softening behaviour.

⁷ Fédération Internationale du Béton

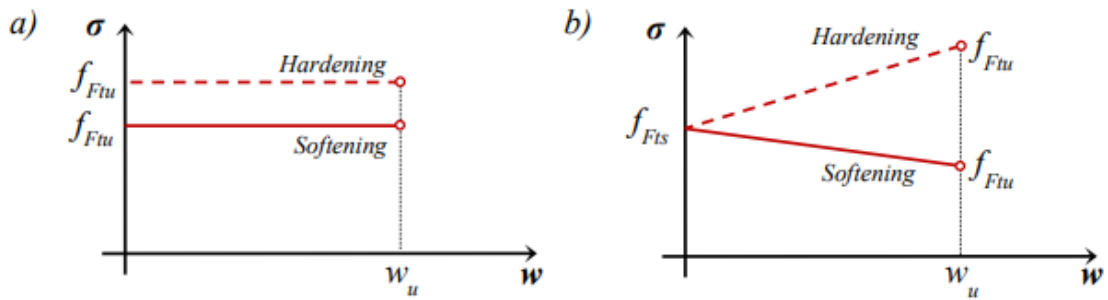


Figure 31 Simplified constitutive laws: a) Rigid-plastic and b) Linear-elastic

The parameters in both diagrams are defined by means of residual flexural tensile strengths, determined in the 3-point bending test EN 14651:2007 [13]. The serviceability residual strength parameter f_{Fts} represents the post-cracking strength for crack openings at SLS. On the other hand, f_{Ftu} represents the ultimate residual strength associated to the ULS crack opening w_u , which is the maximum crack opening accepted in structural design. In the case of rigid-plastic model, the value of w_u is 2.5 mm, whereas for the linear-elastic model, it depends on the ductility required. The equations to determine the parameters f_{Fts} and f_{Ftu} are presented in Table 10.

Table 10 Stress-strain equations according to MC2010

Rigid - plastic	$f_{Ftu} = \frac{f_{R3}}{3}$	$\varepsilon_{ULS} = 20\text{‰} \text{ softening}$ $\varepsilon_{ULS} = 10\text{‰} \text{ hardening}$
Linear - elastic	$f_{Fts} = 0.45 f_{R1}$ $f_{Ftu} = f_{Fts} - \frac{w}{CMOD_3} (f_{Fts} - 0.5f_{R3} + 0.2f_{R1})$ ≥ 0	$\varepsilon_{SLS} = \frac{CMOD_1}{l_{cs}}$ $\varepsilon_{ULS} = \frac{w_u}{l_{cs}} \quad w_u = CMOD_3$

At ULS, the characteristic strength f_{Ftu} must be divided for partial safety coefficients $\gamma_F=1,5$. Nevertheless, residual strength values result to be overestimated [4].

MC2010 is dependent upon the definition of l_{cs} and therefore crack spacing s_m . Crack width evaluations are very sensitive to crack spacing evaluation so it could be easy to make errors which, consequently, can lead to subsequent errors in FRC constitutive law.

Since the two previous shown models are simplifications, the fib Model Code recommends the use of more advanced constitutive laws for numerical analysis.

3.1.2 Rilem

This model is the most reliable and it considers a trilinear σ - ε relation in tension.

The design method was originally developed without size-dependent safety factors. A comparison of the predictions of the design method and of the experimental results of structural elements of various sizes revealed a severe overestimation of the carrying capacity by the design method. In order to compensate this effect, size-dependent safety factors k_h have been introduced [11].

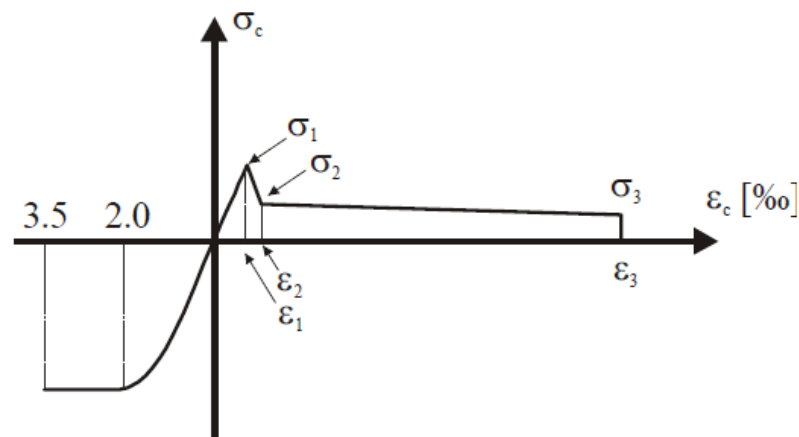


Figure 32 RILEM proposal σ - ε diagram

$$\sigma_1 = 0,7 f_{fctm,fl}(1,6 - d)$$

$$\varepsilon_1 = \frac{\sigma_1}{E_c}$$

$$\sigma_2 = 0,45 f_{R1} k_h$$

$$\varepsilon_2 = \varepsilon_1 + 0.1\text{‰}$$

$$\sigma_3 = 0,37 f_{R4} k_h$$

$$\varepsilon_2 = 25\text{‰}$$

$$E_c = 9500 (f_{fcm})^{1/3}$$

k_h : size factor

$$k_h = 1,0 - 0,6 \frac{h [cm] - 12,5}{47,5} \quad 12,5 \leq h \leq 60 \text{ cm}$$

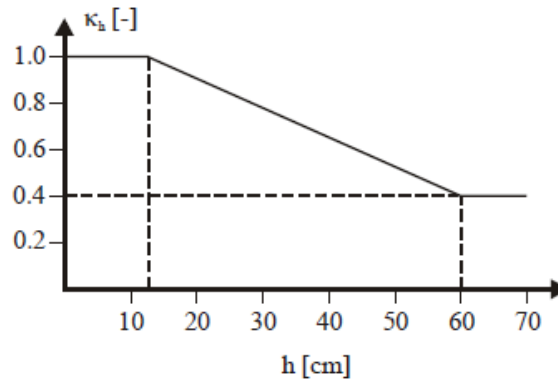


Figure 33 Dependence of the size factor k_h on h

In the following paragraphs, the estimated constitutive law from Rilem method is shown.

3.2 Definition of the constitutive law

It is customary to entrust to concrete a constitutive law characterized only by the branch in compression due to its low ability to react in traction. As it is already said, the addition of fibres represents a great benefit for the structure, since they give tensile strength to cement mixture.

The following paragraph shows how the two constitutive trends are built for FRC behaviour in compression and in tension.

3.2.1 Compression

Among all the usually employed diagrams to represent compression behaviour of concrete, the Sargin's parabola has been considered as the most suitable.

The value of f_{cm} for plain concrete is given by the Table 4. In particular, it is considered a mean value $f_{cm} = 37.5$ MPa.

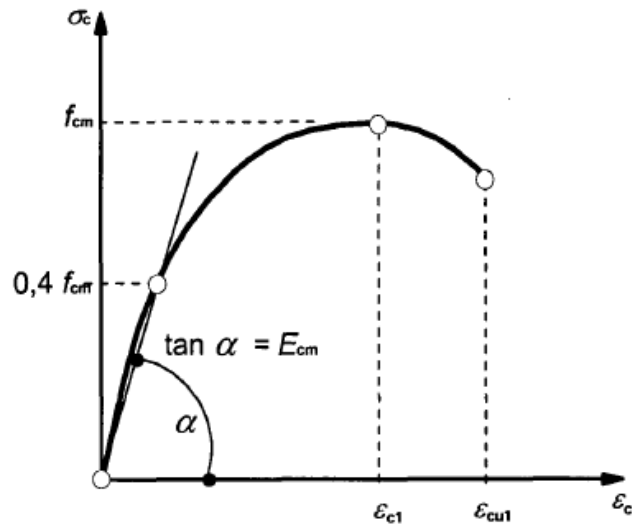


Figure 34 Schematic representation of the stress-strain relation for structural analysis according to EN 1992-1-1:2004 [25]

In accordance to Table 3.1 “Strength and deformation characteristics for concrete” into EN 1992-1-1:2004 [25], also strain at peak stress ϵ_{c1} and the nominal ultimate one ϵ_{cu1} are defined:

$$\epsilon_{c1} = 2.2 \text{ ‰}$$

$$\epsilon_{cu1} = 3.5 \text{ ‰.}$$

As far as the mean strength values for FRC elements concern, they are estimated by Pérez, Groli et al. [2] and they are reported in the Table 11 below.

Table 11 Estimated mean strength values of FRC beams

Beam	Mean strength f_{cm} [MPa]
12-20-0.5%	38.5
12-20-1.0%	39.2
12-70-0.5%	38.9
12-70-1.0%	39.6
25-20-0.5%	39.1
25-20-1.0%	40.0
25-70-0.5%	38.2

25-70-1.0%	38.7
------------	------

3.2.2 Tension

To represent the behaviour in tension, it is applied the Rilem model [11] to the three-point flexural bending test results. The just quoted test has supplied the results already shown in Figure 20 and Figure 21, but it is possible to notice that these are interrupted to $CMOD.3 = 2.5$ mm. In order to apply the Rilem formulation, the trends have been manually extended until the desired $CMOD.4 = 3.5$ mm value, as precisely as possible. The obtained values are presented in Figure 35, Figure 36 and Table 12.

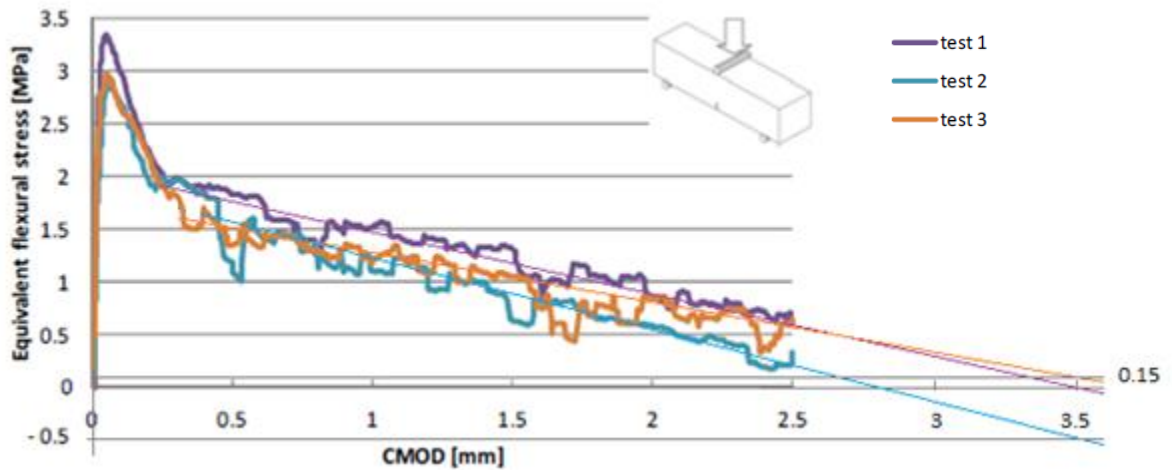


Figure 35 Extrapolation of $CMOD.4$ value from tensile flexural test results for 0.5% in volume of fibre beams

$$f_{Test 1} \approx 0 \text{ MPa}$$

$$f_{Test 2} \approx -0.5 \text{ MPa}$$

$$f_{Test 3} \approx 0.15 \text{ MPa}$$

f_{R4m} is estimated as the average value among the three $CMOD.4$ values:

$$f_{R4m} \approx -0.175 \text{ so it is considered as } 0 \text{ MPa.}$$

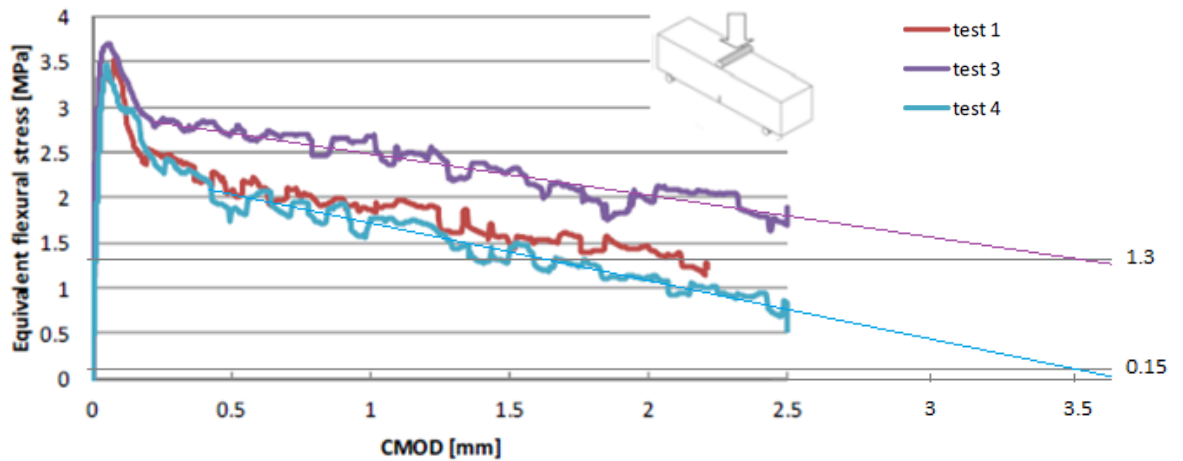


Figure 36 Extrapolation of CMOD.4 value from tensile flexural test results for 1.0% in volume of fibre beams

$f_{\text{Test 1}} \approx 0$ MPa because it stops earlier

$f_{\text{Test 3}} \approx 1.3$ MPa

$f_{\text{Test 4}} \approx 0.15$ MPa

It results that: $f_{R4m} \approx 0.725$ MPa.

A summary of the results in shown below.

Table 12 Equivalent flexural stresses

Tensile residual strength [MPa]					
	LOP ⁸	f_{R1m}	f_{R2m}	f_{R3m}	f_{R4m}
0.5%	3.10	1.53	1.08	0.51	0
1.0%	3.53	2.21	1.72	1.26	0.725

Following the Table 1 of RILEM [11], the mean and characteristic flexural tensile strength of steel fibre reinforced concrete are considered (Table 13).

Table 13 FRC mechanical parameters according to Rilem [11]

f_{fck}	30	MPa
f_{fcm}	38	MPa
$f_{fctk,fl}$	3.4	MPa

⁸ Limit of Proportionality as defined in EN 14651 tensile flexural test

$f_{ctm,fl}$	4.8	MPa
E_{fcm}	32000	MPa

Thanks to the ease on its application and the reliability of the results, the constitutive law is obtained using the Rilem model and the result is represented in Table 14 and Figure 37.

The formulations used are summarized in the paragraph 3.1.2 on page 44.

The size coefficient k_h results to be: $k_h = 0.968$.

Table 14 Tensile strengths according to Rilem [11]

0.5%	σ [MPa]	ϵ
1	4.872	1.52E-04
2	0.667	2.52E-04
3	0.000	0.025

1.0%	σ [MPa]	ϵ
1	4.872	1.52E-04
2	0.963	2.52E-04
3	0.260	0.025

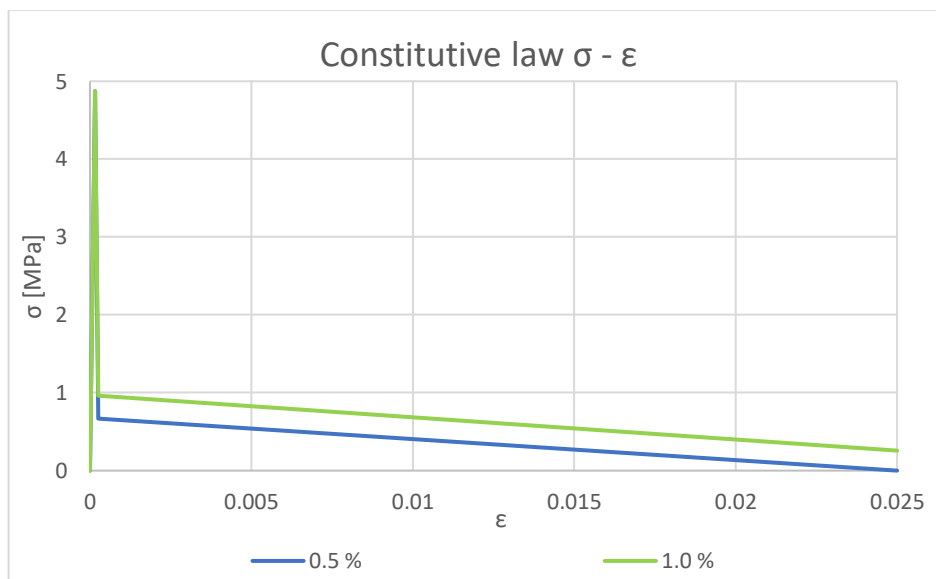


Figure 37 Tensile branch of FRC estimated constitutive law

3.3 Moment – Curvature

The deflection behaviour of a beam can be summarized through the relation Moment-Curvature, M- μ or M- μ -N, of one of its cross-sections. Hypothesizing that, for the De Saint Venant theory, each cross-section remains flat under the action of normal stresses or bending moments, equilibrium (1) and congruence (2) equations can be defined:

$$\text{a) } \int_A \sigma dA = N \quad \text{b) } \int_A \sigma y dA = M + N \cdot e \quad (1)$$

$$\varepsilon = \lambda + \mu \cdot y \quad (2)$$

$$\text{Constitutive law: } \sigma = E \cdot \varepsilon \quad (3)$$

The equations of a beam subjected to axial force or/and bending moment are obtainable using the following equations, defined substituting (2) and (3) into (1a) and (1b):

$$N = E_c(\lambda A_0 + \mu S_0) \quad (4)$$

$$M + N \cdot e = E_c(\lambda S_0 + \mu I_0) \quad (5)$$

Where:

- λ : deformation of the reference origin
- $A_0 = \int_A \frac{E}{E_c} dA \quad S_0 = \int_A \frac{E}{E_c} y dA \quad I_0 = \int_A \frac{E}{E_c} y^2 dA$

Which depend on the geometrical characteristics of the cross-section and on the ratio $n=E_s/E_c$ ⁹.

So, for given values of N and μ , it is possible to obtain λ from the equation (4) and M from (5).

⁹ E_s = steel elastic modulus; E_c = concrete elastic modulus.

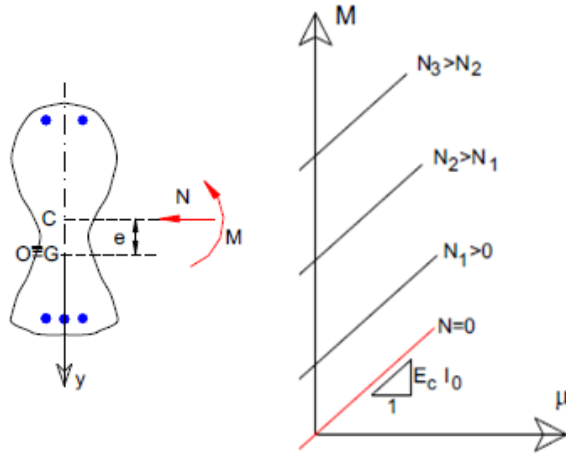


Figure 38 M - μ dependence on N

Actually, due to the non-linearity behaviour of materials, the M - μ diagrams will result to be non-linear too.

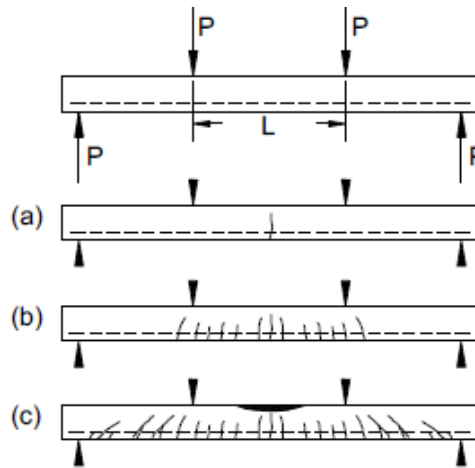


Figure 39 Evolution stages of deformation of a load-bearing beam

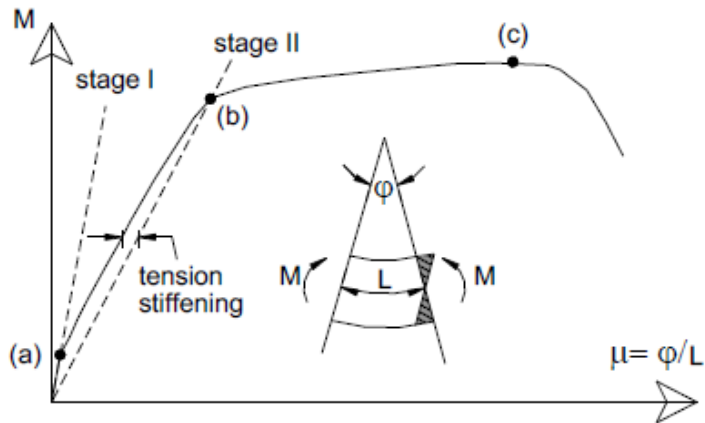


Figure 40 M - μ evolution stages

The representative $M-\mu$ behaviour follows the linear-elastic trend only until the point a) along the “stage I” in Figure 40, where the first crack occurs. In this case, the cross-section is totally reacting. From a) to b), the curve is between the “stage I” and the “stage II”, which defines a linear-elastic relation without tensile contribution of concrete; the cross-section is partialized. This represent the Serviceability Limit State (SLS) and, how it is possible to see from the diagram, tension stiffening is present.

Finally, the Ultimate Limit State (ULS) of the beam is defined between the point b) and the point c).

It follows that a non-linear analysis is necessary to determine $M-\mu$ relation, based on the following hypothesis:

- equilibrium equations: (1a) and (1b);
- congruence equation that defines a strain linear trend: (2);
- perfect adhesion between steel and concrete;
- non-linear $\sigma-\varepsilon$ relation for steel and concrete: $\sigma \neq E \cdot \varepsilon$.

Equations (1a), (1b) and (2) constitute the non-linear system:

$$a) \int_A \sigma(\lambda + \mu \cdot y) dA = N \quad b) \int_A \sigma(\lambda + \mu \cdot y) y dA = M + N \cdot e \quad (6)$$

In order to solve it, it is usually performed a numerical analysis supposing the cross-section as subdivided in infinitesimal strips of area dA .

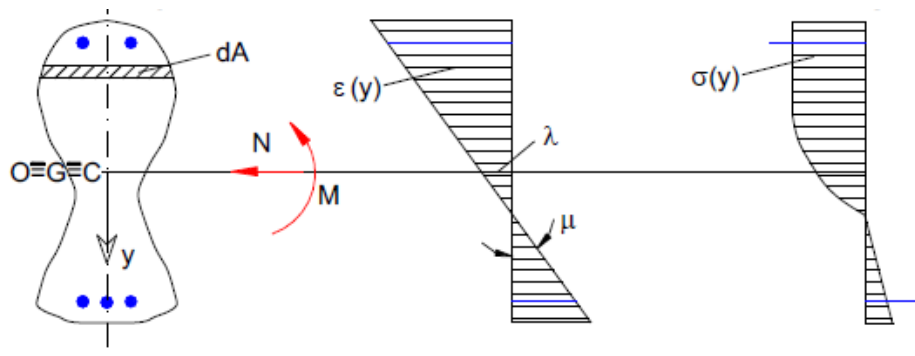


Figure 41 Stress and strain development for non-linear analysis

For given μ and N values, M is obtained:

- 1) supposing a value of λ ;
- 2) definition of strain state through (2);
- 3) stress state definition using the constitutive law σ - ϵ of materials;
- 4) N_t through the equation (6a);
- 5) If $N_t \neq N$, the process has to be done again with a new value of λ ;
- 6) If $N_t = N$, M can be defined using the equation (6b).

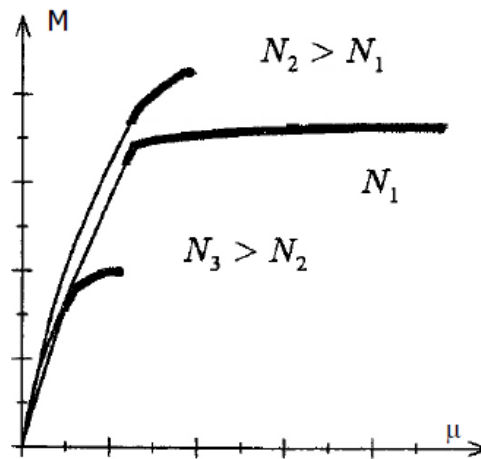


Figure 42 Numerical procedure for the definition of M

Another option to compute this M - μ relation is represented by using a program, that is what it has been chosen for this work. Geometrical properties, reinforcement quantities and mechanical parameters have allowed to easily determine M - μ diagrams for each FRC beam. The interest will be only on the negative curve because of the configuration of the test. The asymmetry of the curves is due to the non-symmetry of reinforcements in compression and tension area of the cross-section.

The Moment-Curvature diagrams obtained are in the paragraph 9.1 of “Chapter 9: Annex”.

3.4 Computation of the Deflection

The final step consists in determining the mid-span deflection η . There are several methods to reach this aim, but the one chosen is the Principal of Virtual Works (PVW).

$$U \cdot \eta = \int_L \frac{M_a M_b}{EI} = \int_L M_a \mu_b dz$$

$$\eta = \frac{2}{U} \int_0^{L/2} M_a \mu_b dz$$

- M_a is the moment produced by the virtual system where a unit load U is applied in the centre of the span;
- M_b is the moment given by the external loads applied at the cantilever edges and μ_b is the respective curvature;
- L is the length of the beam and, thanks to the symmetry of the geometry, the integral is extended only to half of the length and then multiplied by 2.

M_a has a triangular shape that characterizes only the middle span; all along the cantilever regions, the moment is null (Figure 43 and Figure 44).

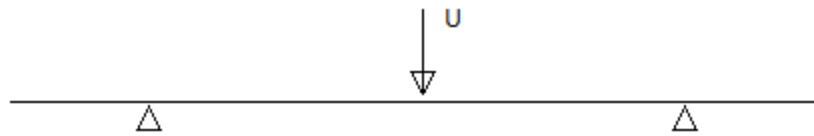


Figure 43 Virtual system of PVW



Figure 44 M_a : moment given by U

M_b is characterized by two contributes:

- The external applied loads;
- The self-weight of the beam.

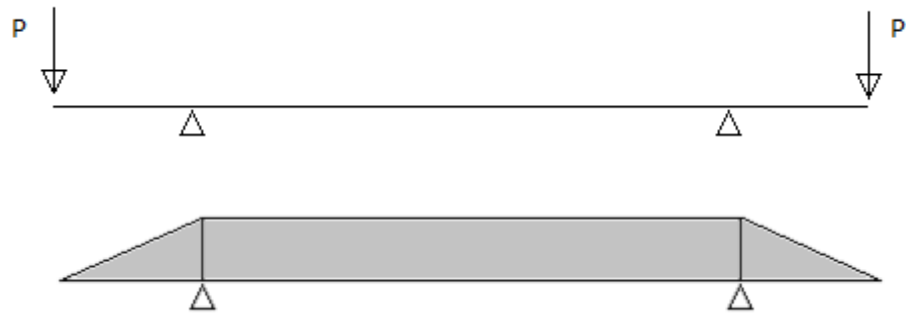


Figure 45 Moment diagram due to external loads

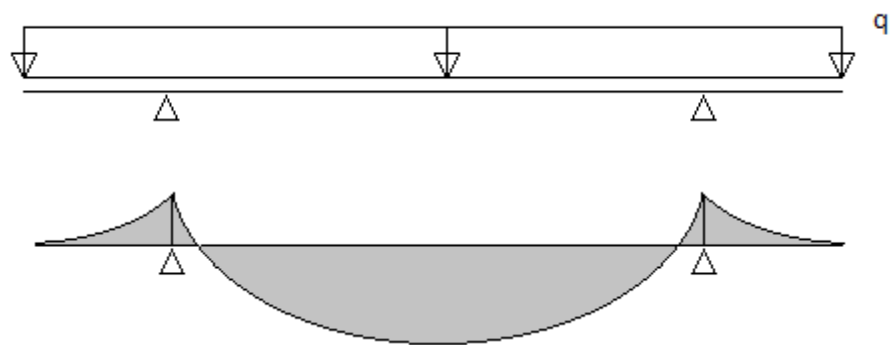


Figure 46 Moment diagram due to self-weight

The definition of M_b is necessary to obtain the corresponding curvature μ_b through the previous Moment-Curvature diagrams, which have been linearized with two, three or four branches as necessary, in order to facilitate the interpolation.

4 Results

The ultimate load values are considered for each beam, given by Groli [2] and clearly visible in the experimental results shown in Table 7, Figure 24, Figure 25, Figure 26 and Figure 27, and they are divided in twenty intervals in order to find twenty corresponding values of curvature to consequently compare with the empirical results.

The proposed Model, in fact, gives directly in output the value of the deflection by inserting the value of the load.

Surely, it would have been possible to define an even more detailed and precise model considering a higher number of ranges.

Table 15 Load-Deflection from numerical Model of 12-20-ZZ and 12-70-ZZ beams

12-20-0.5%		12-20-1.0%		12-70-0.5%		12-70-1.0%	
P	η	P	η	P	η	P	η
kN	mm	kN	mm	kN	mm	kN	mm
0	0	0	0	0	0	0	0
10.5	0.220	10.9	0.264	9.8	0.081	10.4	0.076
21.0	0.634	21.8	0.745	19.5	0.245	20.7	0.222
31.5	1.047	32.7	1.225	29.3	0.408	31.1	0.367
42.0	1.461	43.6	1.706	39.0	0.572	41.4	0.513
52.5	1.875	54.5	2.187	48.8	0.736	51.8	0.658
63.0	2.289	65.4	2.668	58.5	0.904	62.1	0.933
73.5	2.983	76.3	3.181	68.3	1.977	72.5	2.495
84.0	4.203	87.2	4.300	78.0	3.628	82.8	4.078
94.5	5.423	98.1	5.465	87.8	5.278	93.2	5.661
105.0	6.643	109.0	6.631	97.5	6.929	103.5	7.244
115.5	7.863	119.9	7.796	107.3	8.579	113.9	8.827
126.0	9.083	130.8	8.961	117.0	10.230	124.2	10.411

The effect of recycled steel fibres on the deflection of reinforced concrete beams

136.5	10.303	141.7	10.126	126.8	11.881	134.6	11.994
147.0	11.523	152.6	11.292	136.5	13.531	144.9	13.577
157.5	12.743	163.5	12.457	146.3	15.183	155.3	15.160
168.0	14.980	174.4	13.664	156.0	19.231	165.6	18.696
178.5	22.314	185.3	18.180	165.8	26.286	176.0	26.359
189.0	48.618	196.2	23.759	175.5	85.206	186.3	83.817
199.5	196.890	207.1	55.908	185.3	188.927	196.7	187.394
210.0	345.161	218.0	194.336	195.0	292.648	207.0	290.970

Table 16 Load-Deflection from numerical Model of 25-20-ZZ and 25-70-ZZ beams

25-20-0.5%		25-20-1.0%		25-70-0.5%		25-70-1.0%	
P	η	P	η	P	η	P	η
kN	mm	kN	mm	kN	mm	kN	mm
0	0	0	0	0	0	0	0
29.4	0.844	29.5	0.847	26.0	0.345	23.2	0.299
58.7	1.859	59.0	1.864	51.9	0.770	46.4	0.679
88.1	2.873	88.5	2.880	77.9	1.218	69.6	1.058
117.4	3.887	118.0	3.897	103.8	2.580	92.8	1.880
146.8	4.901	147.5	4.913	129.8	3.965	116.0	3.112
176.1	5.916	177.0	5.930	155.7	5.349	139.2	4.344
205.5	6.930	206.5	6.946	181.7	6.734	162.4	5.577
234.8	7.944	236.0	7.963	207.6	8.118	185.6	6.809
264.2	8.958	265.5	8.980	233.6	9.503	208.8	8.041
293.5	9.973	295.0	9.996	259.5	10.887	232.0	9.274
322.9	10.987	324.5	11.013	285.5	12.272	255.2	10.506
352.2	12.001	354.0	12.029	311.4	13.656	278.4	11.738
381.6	13.015	383.5	13.046	337.4	15.041	301.6	12.971
410.9	14.030	413.0	14.062	363.3	16.425	324.8	14.203
440.3	15.044	442.5	15.079	389.3	17.810	348.0	15.436
469.6	16.058	472.0	16.096	415.2	19.194	371.2	16.668
499.0	17.073	501.5	17.112	441.2	20.579	394.4	17.900
528.3	23.726	531.0	18.129	467.1	27.362	417.6	19.133
557.7	39.283	560.5	28.706	493.1	40.914	440.8	20.365
587.0	54.841	590.0	43.209	519.0	54.466	464.0	21.617

The effect of recycled steel fibres on the deflection of reinforced concrete beams

Table 17 Load-Deflection from numerical Model of no fibres and no stirrups beams

12-20-00 WF		12-70-00 WF		25-20-00 WF		25-70-00 WF	
P	η	P	η	P	η	P	η
kN	mm	kN	mm	kN	mm	kN	mm
0	0	0	0	0	0	0	0
9.2	0.406	7.4	0.310	24.0	0.681	21.8	0.842
18.4	1.279	14.8	1.234	48.0	1.537	43.7	1.928
27.6	2.152	22.2	2.158	72.0	2.394	65.5	3.015
36.8	3.024	29.6	3.082	96.0	3.250	87.3	4.102
46.0	3.897	37.0	4.006	120.0	4.107	109.1	5.188
55.2	4.770	44.4	4.930	144.0	4.963	131.0	6.275
64.4	5.643	51.8	5.854	168.0	5.820	152.8	7.362
73.6	6.516	59.2	6.778	192.0	6.676	174.6	8.448
82.8	7.388	66.6	7.702	216.0	7.533	196.4	9.535
92.0	8.261	74.0	8.626	240.0	8.389	218.3	10.621
101.2	9.134	81.4	9.550	264.0	9.246	240.1	11.708
110.4	10.007	88.8	10.474	288.0	10.102	261.9	12.795
119.6	10.880	96.2	11.398	312.0	10.959	283.7	13.881
128.8	11.753	103.6	12.322	336.0	11.815	305.6	14.968
138.0	12.633	111.0	13.246	360.0	12.672	327.4	16.055
147.2	15.979	118.4	14.170	384.0	13.528	349.2	17.141
156.4	21.467	125.8	15.121	408.0	14.384	371.0	18.228
165.6	29.280	133.2	18.186	432.0	15.241	392.9	19.315
174.8	82.552	140.6	22.979	456.0	16.097	414.7	20.401
184.0	141.981	148.0	28.828	480.0	16.954	436.5	21.519

Table 18 Load-Deflection from numerical Model of beams with stirrups spacing of 10 cm and no fibres

12-20-10 WF		12-70-10 WF		25-20-10 WF		25-70-10 WF	
P	η	P	η	P	η	P	η
kN	mm	kN	mm	kN	mm	kN	mm
0	0	0	0	0	0	0	0
9.8	0.464	8.6	0.460	27.2	0.795	22.1	0.857
19.6	1.394	17.2	1.533	54.4	1.765	44.3	1.959
29.4	2.325	25.8	2.607	81.6	2.735	66.4	3.061
39.2	3.255	34.4	3.681	108.8	3.706	88.5	4.162
49.0	4.186	43.0	4.755	136.0	4.676	110.7	5.264
58.8	5.116	51.6	5.829	163.1	5.646	132.8	6.366
68.7	6.047	60.2	6.903	190.3	6.617	154.9	7.468

The effect of recycled steel fibres on the deflection of reinforced concrete beams

78.5	6.977	68.8	7.976	217.5	7.587	177.0	8.570
88.3	7.908	77.4	9.050	244.7	8.557	199.2	9.672
98.1	8.838	86.0	10.124	271.9	9.528	221.3	10.773
107.9	9.769	94.6	11.198	299.1	10.498	243.4	11.875
117.7	10.699	103.2	12.272	326.3	11.468	265.6	12.977
127.5	11.724	111.8	13.346	353.5	12.439	287.7	14.079
137.3	12.562	120.4	14.420	380.7	13.409	309.8	15.181
147.1	15.932	129.0	15.792	407.9	14.379	332.0	16.283
156.9	21.782	137.6	21.036	435.0	15.349	354.1	17.384
166.7	32.226	146.2	26.881	462.2	16.320	376.2	18.486
176.5	93.818	154.8	50.723	489.4	17.290	398.3	19.588
186.4	157.174	163.4	83.420	516.6	21.755	420.5	20.690
196.2	220.529	172.0	116.116	543.8	35.080	442.6	23.279

Table 19 Load-Deflection from numerical Model of beams with stirrups spacing of 30 cm and no fibres

12-20-30 WF		12-70-30 WF		25-20-30 WF		25-70-30 WF	
P	η	P	η	P	η	P	η
kN	mm	kN	mm	kN	mm	kN	mm
0	0	0	0	0	0	0	0
9.7	0.449	7.9	0.375	24.3	0.691	20.1	0.756
19.3	1.364	15.8	1.364	48.6	1.557	40.2	1.757
29.0	2.280	23.8	2.352	72.8	2.423	60.3	2.757
38.6	3.195	31.7	3.341	97.1	3.290	80.4	3.758
48.3	4.111	39.6	4.330	121.4	4.156	100.5	4.759
57.9	5.026	47.5	5.319	145.7	5.022	120.6	5.760
67.6	5.942	55.4	6.308	169.9	5.888	140.7	6.760
77.2	6.857	63.4	7.297	194.2	6.755	160.8	7.761
86.9	7.773	71.3	8.286	218.5	7.621	180.9	8.762
96.5	8.688	79.2	9.275	242.8	8.487	201.0	9.763
106.2	9.604	87.1	10.264	267.0	9.354	221.1	10.763
115.8	10.519	95.0	11.253	291.3	10.220	241.2	11.764
125.5	11.435	103.0	12.242	315.6	11.086	261.3	12.765
135.1	12.350	110.9	13.231	339.9	11.952	281.4	13.766
144.8	14.518	118.8	14.220	364.1	12.819	301.5	14.766
154.4	20.274	126.7	15.272	388.4	13.685	321.6	15.767
164.1	26.820	134.6	19.119	412.7	14.551	341.7	16.768
173.7	75.447	142.6	24.249	437.0	15.418	361.8	17.769
183.4	137.782	150.5	34.299	461.2	16.284	381.9	18.769

193.0	200.117	158.4	64.410	485.5	17.150	402.0	19.770
-------	---------	-------	--------	-------	--------	-------	--------

4.1 Comparison between numerical and experimental results

The results obtained through the model are then compared with the ones achieved in laboratory by Pérez et al. with Load-Deflection representations.

The Figures attached into “Annex” (paragraph 9.2) show a great reliability of the results obtained and the compatibility among the values given by the model and the empirical experience, especially in the serviceability phase. For the purpose of this thesis, in fact, the attention is focused in the SLS.

4.2 Analysis of the results

The credibility of the values given by the model has allowed, therefore, to utilize it to theorize the behaviour of beams with different characteristics and to compare their distinct behaviour.

It is worthy to point out the following results, where Load-Deflection relations of FRC beams and RC beams are plotted and compared with each other. As reference for non-fibre reinforced elements, beams with stirrups spacing of 10 cm are considered. In fact, the presence of shear reinforcement does not lead to changes in deflection behaviour, but rather affects confinement effects, which are not object of study of this thesis.

The effect of recycled steel fibres on the deflection of reinforced concrete beams

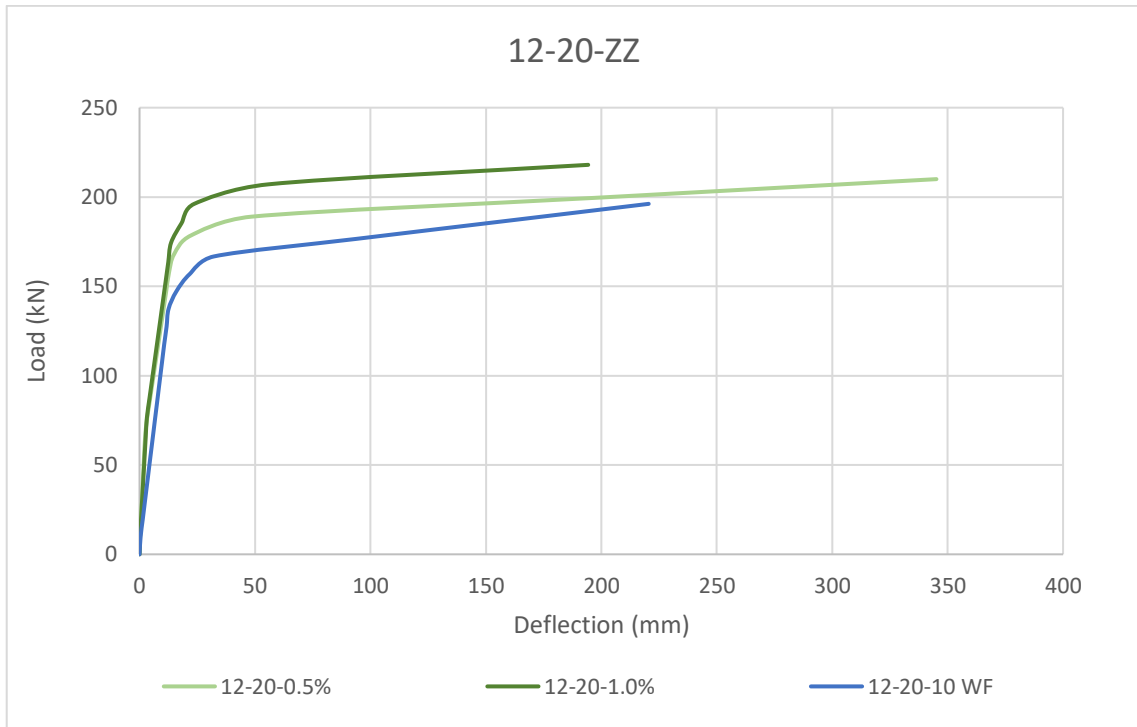


Figure 47 P- η results from numerical model: comparison among FRC and RC beams with $\varnothing 12$ rebars and $c=20$ mm

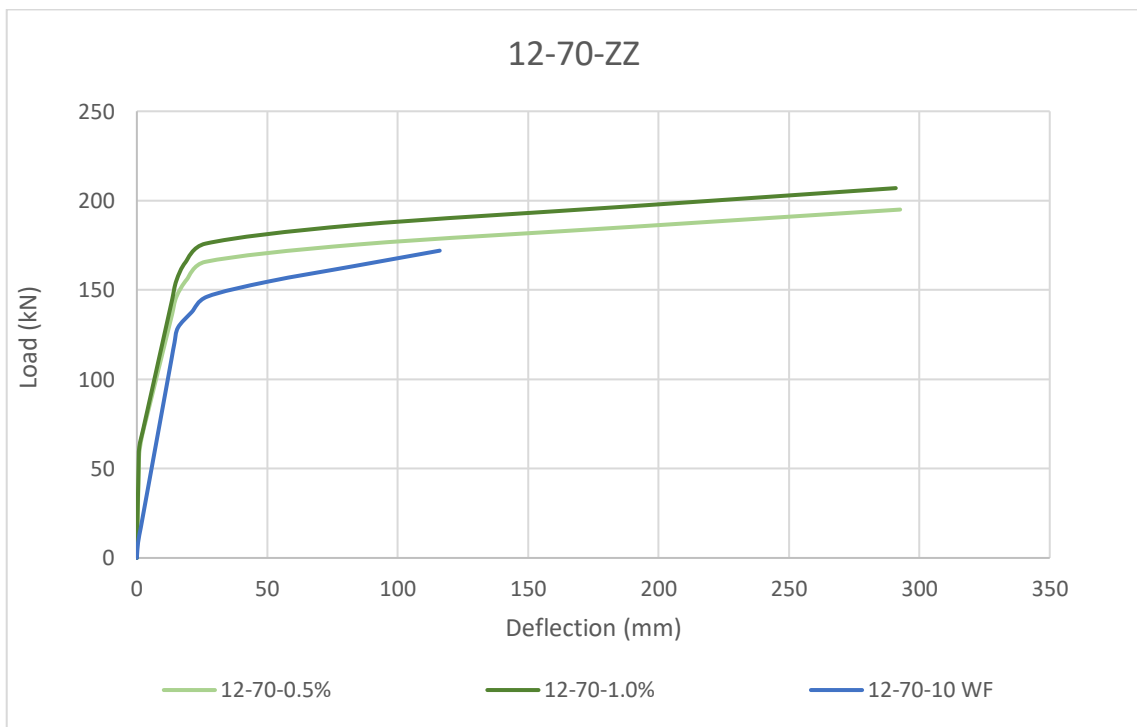


Figure 48 P- η results from numerical model: comparison among FRC and RC beams with $\varnothing 12$ rebars and $c=70$ mm

The effect of recycled steel fibres on the deflection of reinforced concrete beams

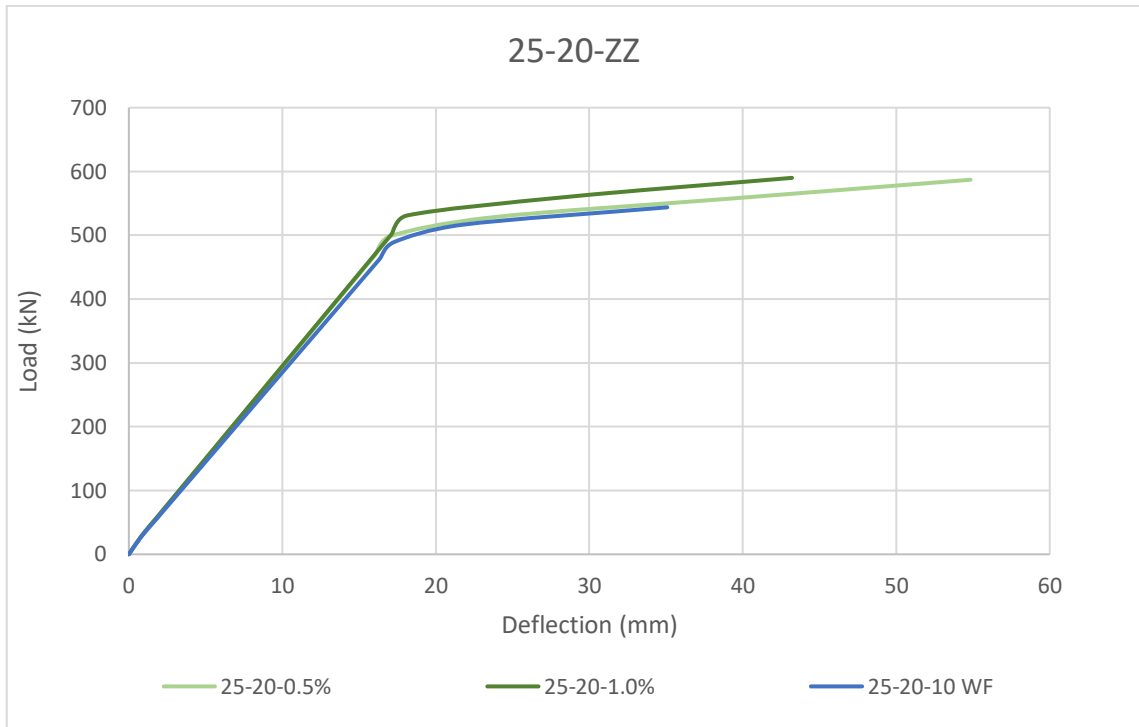


Figure 49 P- η results from numerical model: comparison among FRC and RC beams with $\text{Ø}25$ rebars and $c=20$ mm

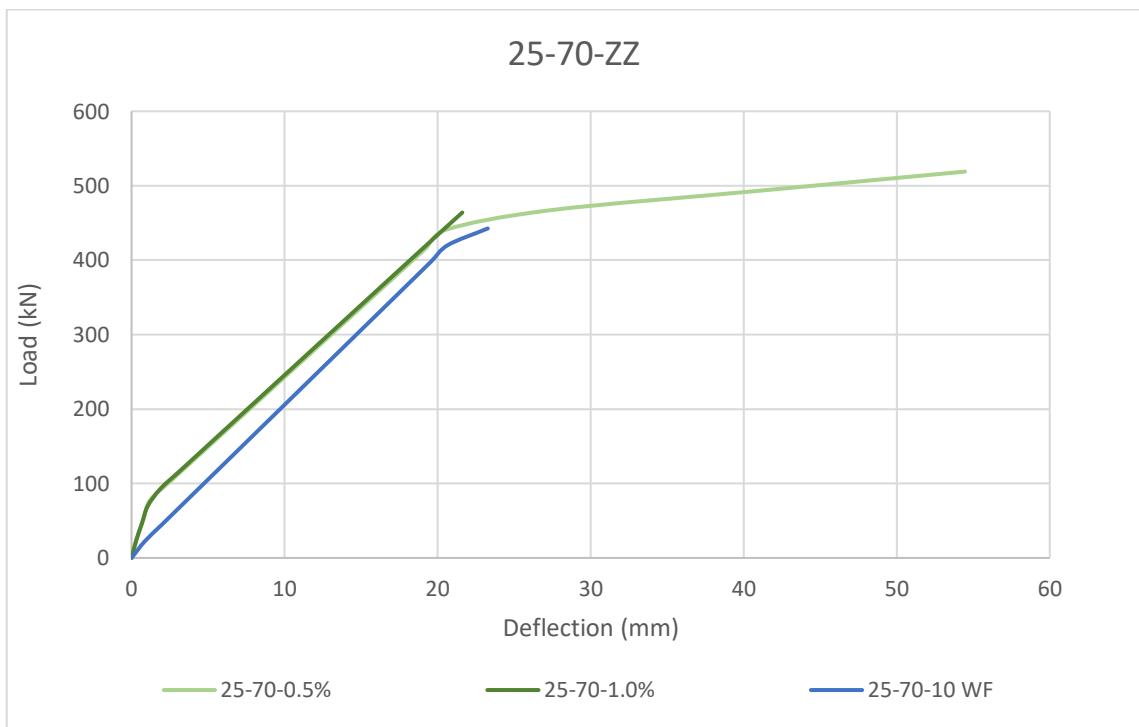


Figure 50 P- η results from numerical model: comparison among FRC and RC beams with $\text{Ø}25$ rebars and $c=70$ mm

As expected, what it emerges from the previous graphs is that the presence of fibres entails a better resistance to loads by the beam. A close-up of the serviceability region of the previous plots are done to make in evidence this thesis. In particular, the comparison among the values of the load are done considering fixed values of the deflection, assumed to be the limit ones:

$$\eta_{LIM,1} = \frac{L}{500} = 9.84 \text{ mm}$$

$$\eta_{LIM,2} = \frac{L}{250} = 19.68 \text{ mm}$$

Table 20 Comparison of load values of FRC and RC beams for fixed values of the deflection

12-20-ZZ	P [kN]	
η_{LIM}	9.84	19.68
12-20-10	108.64	153.40
12-20-0.5%	132.52	174.73
12-20-1.0%	139.02	188.23

12-70-ZZ	P [kN]	
η_{LIM}	9.84	19.68
12-70-10	83.72	135.37
12-70-0.5%	114.70	156.62
12-70-1.0%	120.47	166.93

25-20-ZZ	P [kN]	
η_{LIM}	9.84	19.68
25-20-10	280.66	503.97
25-20-0.5%	289.66	510.45
25-20-1.0%	290.47	535.33

25-70-ZZ	P [kN]	
η_{LIM}	9.84	19.68
25-70-10	202.55	400.18
25-70-0.5%	239.87	424.30

25-70-1.0%	242.66	427.90
------------	--------	--------

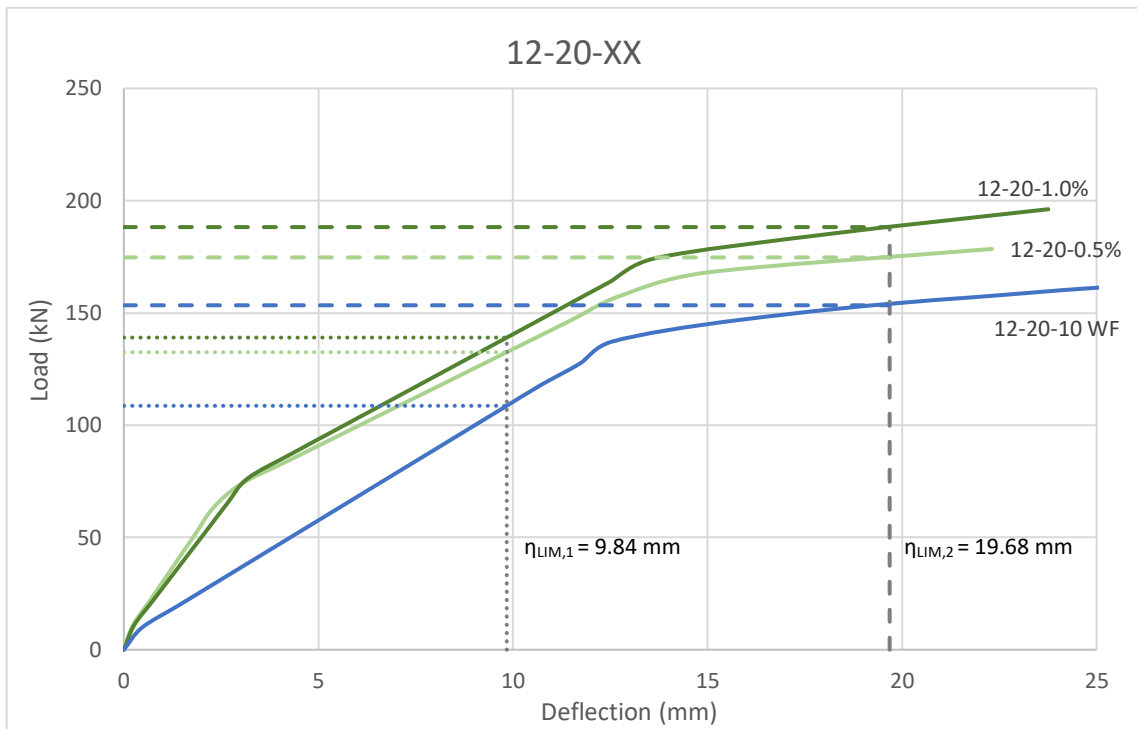


Figure 51 Close-up of Figure 47 in serviceability region

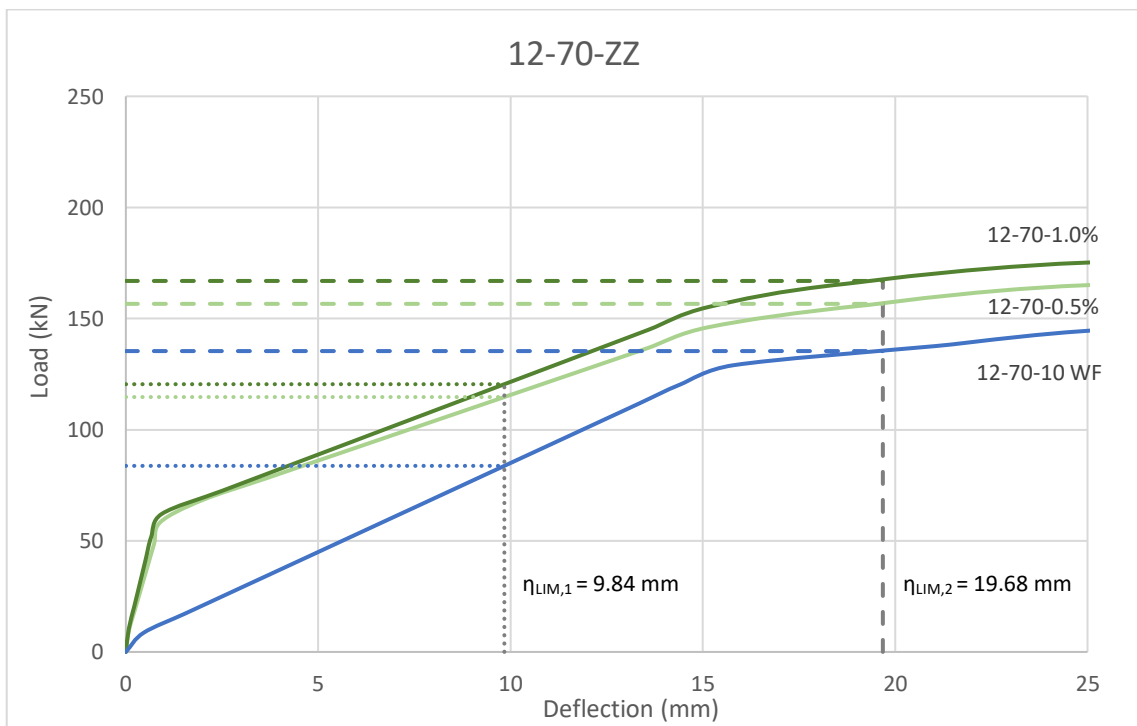


Figure 52 Close-up of Figure 48 in serviceability region

The effect of recycled steel fibres on the deflection of reinforced concrete beams

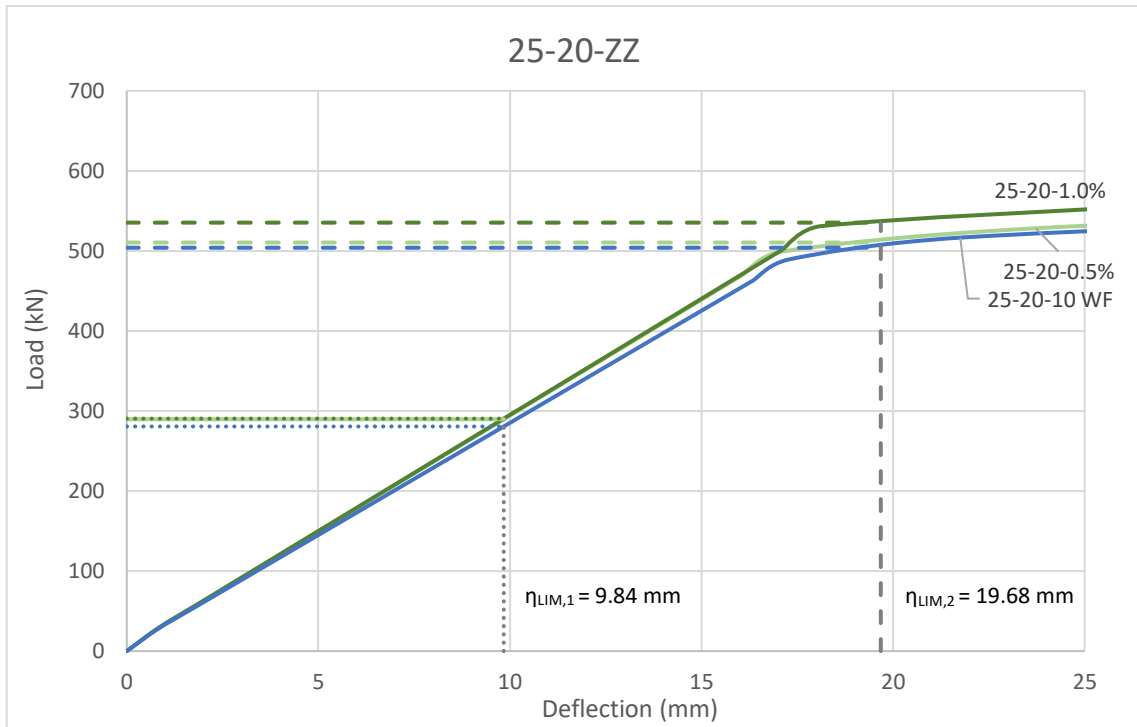


Figure 53 Close-up of Figure 49 in serviceability region

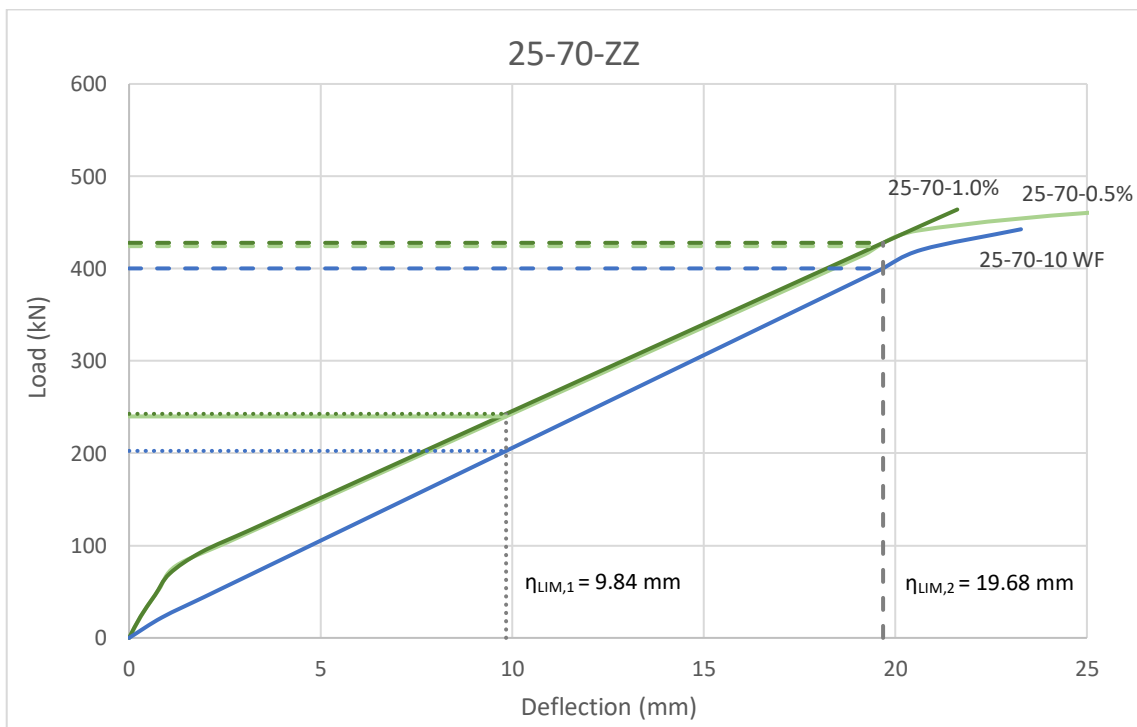


Figure 54 Close-up of Figure 50 in serviceability region

Together with the conclusion previously explained, from the aforementioned diagrams, it seems to emerge that the increase of load is greater in the case of smaller reinforcement. With this idea in mind, some diagrams are represented with the purpose of verifying it.

The percentage of tensile reinforcement, equal to 0.29% for rebars with diameter of 12 mm and 1.25% for Ø25 ones, is plotted with respect to the load increment for the same fixed deflection limits previously mentioned:

$$\eta_{LIM,1} = \frac{L}{500} = 9.84 \text{ mm}$$

$$\eta_{LIM,2} = \frac{L}{250} = 19.68 \text{ mm}$$

Results for fixed $\eta_{LIM,1}$

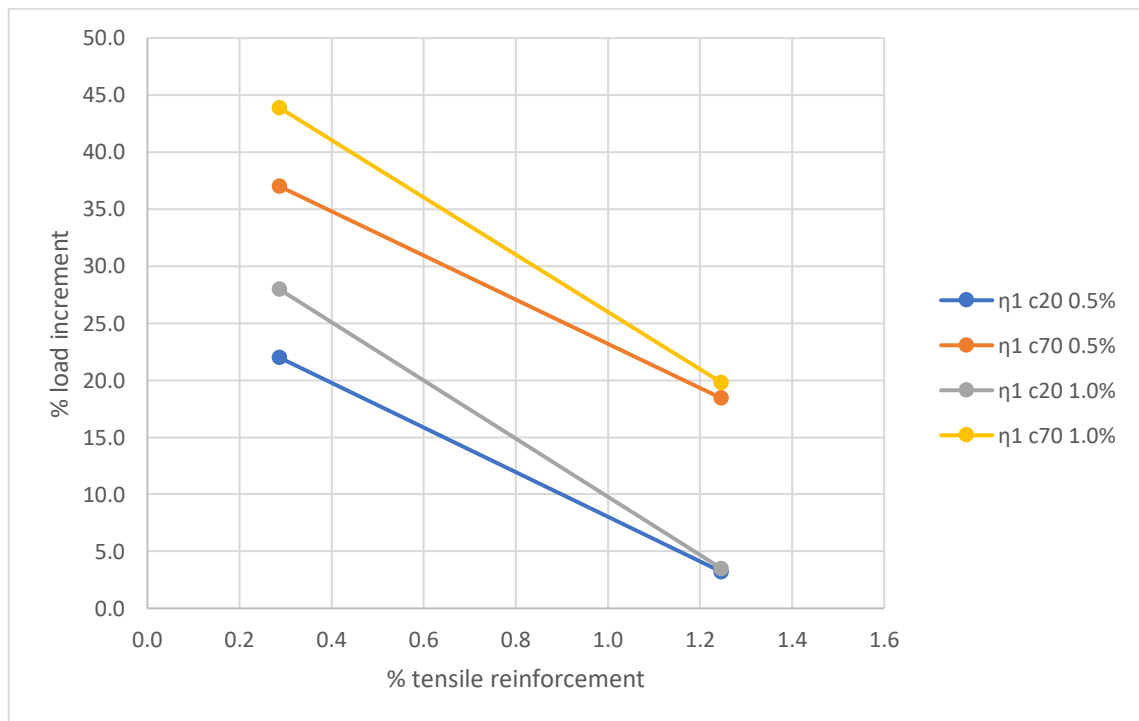


Figure 55 % tensile reinforcement with respect to % load increment for $\eta_{LIM,1}$

The effect of recycled steel fibres on the deflection of reinforced concrete beams

Table 21 % tensile reinforcement with respect to % load increment for $\eta_{LIM,1}$

$\eta_{LIM,1}$	Fibre	Concrete cover [mm]	Tensile reinforcement [%]	Load increment [%]
	0.5%	20	0.29	21.98
			1.25	3.21
		70	0.29	36.99
			1.25	18.42
	1.0%	20	0.29	27.96
			1.25	3.50
		70	0.29	43.89
1.25			19.80	

Results for fixed $\eta_{LIM,2}$

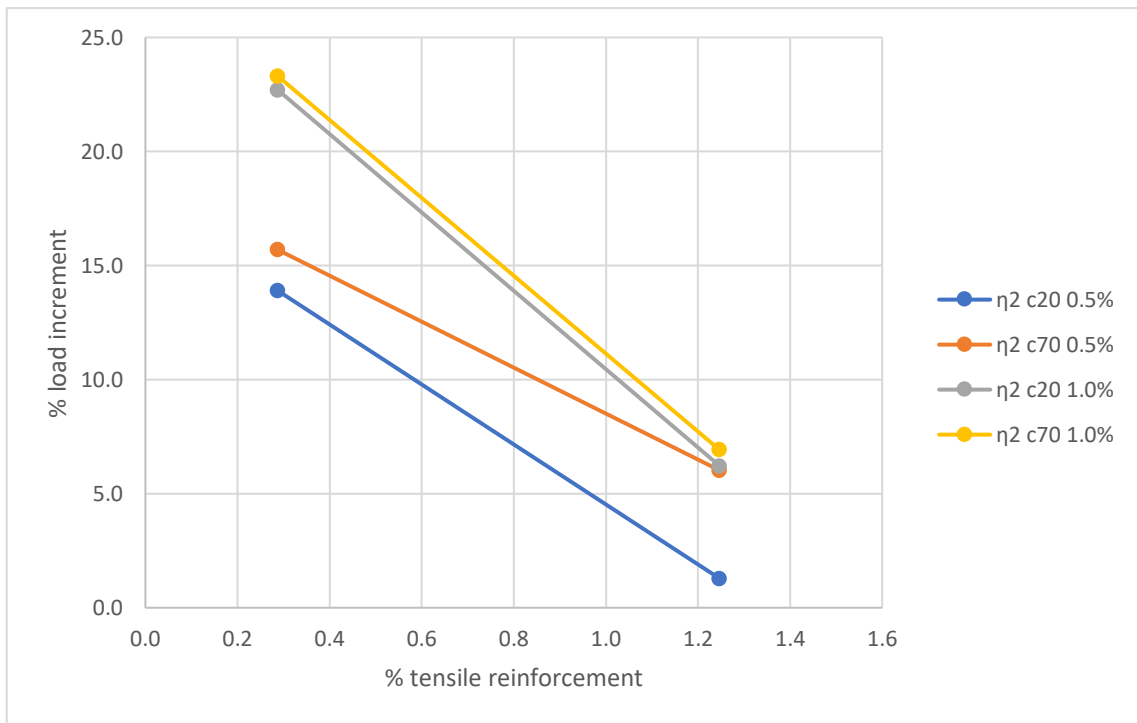


Figure 5 % tensile reinforcement with respect to % load increment for $\eta_{LIM,2}$

The effect of recycled steel fibres on the deflection of reinforced concrete beams

Table 22 % tensile reinforcement with respect to % load increment for $\eta_{LIM,2}$

	Fibre	Concrete cover [mm]	Tensile reinforcement [%]	Load increment [%]
$\eta_{LIM,2}$	0.5%	20	0.29	13.90
			1.25	1.29
		70	0.29	15.69
			1.25	6.03
	1.0%	20	0.29	22.70
			1.25	6.22
		70	0.29	23.31
			1.25	6.93

5 Conclusions

The present thesis has dealt with elements made by self-compactable concrete (SCC) reinforced with conventional steel rebars to which recycled steel fibres have been incorporated. The general idea that arose from the study is that conventional reinforcement cannot be replaced by fibres, since they do not substantially increase tensile strength of concrete. Nevertheless, their contribute is not negligible and they have demonstrated to achieve the attended results.

However, before analysing the more engineering aspects linked to the employment of Recycled Steel Fibres (RSF), it is worthy to underline the reason behind the choice of such a material instead of commercial steel fibres. Thanks to the results of Groli et al. [2], it is proved the feasibility of using RSF from End-of-Life tires and, through their experimental campaign, the problem of finding the optimum concrete mix needed to guarantee workability has been overcome. This has allowed to benefit from the use of a recycled material and thus bring improvements in terms of sustainability. In fact, RSFs represent a great advantage economically speaking and, above all, they are a material with a very reduced environmental impact.

As far as the Model created concerns, from Figure 65 to Figure 72 (into “Annex”), it is possible to see the trend of Load-Deflection obtained with the numerical Model compared to the real one achieved in laboratory. It is evident how they perfectly match in the serviceability phase while they move slightly away going towards the ultimate state. Thus, its trustworthiness allows to consider it validated.

This result let represent through the model not only the deflection behaviour of FRC beams, but also the simply reinforced beams one, as in **Errore. L'origine riferimento non è stata trovata.**, Figure 48, Figure 49, Figure 50 and from these curves, it is possible

to point out that higher the amount of fibre in volume, higher the load that the beams are able to support. Moreover, a close-up of these plots (see from **Errore. L'origine riferimento non è stata trovata.** to Figure 54) confirms the just explained thesis showing in a very clear way the results for fixed deflection limits.

Looking at these results, some other considerations come: in fact, it is evident the relation between the percentage of load increment and the percentage of reinforcement into the beams. Plotting this data (see Figure 55 and Figure 56), very important results emerged: the contribute of fibres is more evident when the percentage of reinforcement into the beam is lower. In fact, what it is evident from the graphs is that the load increment rises if:

- The quantity of tensile reinforcement decreases;
- The concrete cover grows;
- The fibre content increases.

All the explained aspects permit to conclude that the employment of recycled steel fibres in low to moderate content, with the combined action of rebars, improves tension stiffening of concrete leading to an enhancement of the mechanical behaviour of the material. In terms of deflection, that is the main object of this work, they contribute to reduce the deformation under the same load and to parity of beam length.

Thinking on defining the load starting from fixed deflection values, that are identified as the limit ones $L/250$ and $L/500$, the model has been fundamental to interpret the experimental results and to reach the most important conclusion: assuming that the beam has reached the deflection value supposed, in order to obtain the same load given in the case of no fibre reinforced beams, it is necessary to reduce the cross-section, to use shorter beams or to put less reinforcement rebars. So, it is possible to save material in order to achieve the same performance in service, for instance, reducing the cross-sections and so increasing the sustainability.

Finally, all these considerations are strictly connected to the production process of concrete, as already mentioned in the Introduction: minimize concrete consumption will help mitigate the effect of concrete industry on CO_2 production and so on climate change.

6 Figure Index

Figure 1 Production process of cement.....	7
Figure 2 Examples of fibres' materials.....	8
Figure 3. Some type of available steel fibres.....	9
Figure 4 Recycled rubber in various sizes	10
Figure 5 Recycled steel fibres from End-of-Life tyres	11
Figure 6 Comparison between emitted CO ₂ kgs to obtain one ton of new steel fibres from scrap steel and process the recycled ones for direct use	12
Figure 7 Direct tensile test on a) bone and b) cylinder specimens	17
Figure 8 Notched specimen	18
Figure 9 Attended results for notched specimens	18
Figure 10 Non-notched specimen	18
Figure 11 Attended results for specimens without notch	19
Figure 12 Tensile flexural specimen according to ASTM C1609/1609M	19
Figure 13 Attended results of 4-point bending tensile flexural test.....	20
Figure 14 Possible P- η behaviour depending on reinforcement.....	21
Figure 15 Tensile flexural specimen according to EN 14651.....	22
Figure 16 Details of tensile flexural specimen	22
Figure 17 Typical Load-CMOD diagram	23

Figure 18 Fibres used in preliminary study: a) recycled short, series TR; b) recycled long, series R; c) commercial hooked, series CH; d) commercial straight, series C [2]	25
Figure 19 Comparison of 3-point tensile flexural tests. Green curves are for recycled fibres, while black ones are for commercial steel fibres [2].....	27
Figure 20 Results of tensile flexural test for specimens with 0.5% in volume of fibre..	29
Figure 21 Results of tensile flexural test for specimens with 1.0% in volume of fibre..	29
Figure 22 Cross-sections of the analysed beams (dimensions in mm); ZZ is the fibre content: 0%, 0.5% or 1.0%	31
Figure 23 Four-point flexural bending test set-up	31
Figure 24 Load-deflection for 12-20-ZZ beams	33
Figure 25 Load-deflection for 12-70-ZZ beams	33
Figure 26 Load-deflection for 25-20-ZZ beams	34
Figure 27 Load-deflection for 25-70-ZZ beams	34
Figure 28 Stress-strain and stress- crack width models.....	41
Figure 29 Structural characteristic length according to MC2010 [2]	41
Figure 30 Definition of "y" for a) sections with traditional reinforcement and b) sections without traditional reinforcement [2].....	42
Figure 31 Simplified constitutive laws: a) Rigid-plastic and b) Linear-elastic	43
Figure 32 RILEM proposal σ - ϵ diagram.....	44
Figure 33 Dependence of the size factor k_h on h	45
Figure 34 Schematic representation of the stress-strain relation for structural analysis according to EN 1992-1-1:2004 [25].....	46
Figure 35 Extrapolation of CMOD.4 value from tensile flexural test results for 0.5% in volume of fibre beams	47
Figure 36 Extrapolation of CMOD.4 value from tensile flexural test results for 1.0% in volume of fibre beams	48
Figure 37 Tensile branch of FRC estimated constitutive law.....	49

Figure 38 M- μ dependence on N	51
Figure 39 Evolution stages of deformation of a load-bearing beam.....	51
Figure 40 M- μ evolution stages	51
Figure 41 Stress and strain development for non-linear analysis	52
Figure 42 Numerical procedure for the definition of M	53
Figure 43 Virtual system of PVW	54
Figure 44 M_a : moment given by U.....	54
Figure 45 Moment diagram due to external loads	55
Figure 46 Moment diagram due to self-weight.....	55
Figure 47 P- η results from numerical model: comparison among FRC and RC beams with Ø12 rebars and c=20 mm.....	61
Figure 48 P- η results from numerical model: comparison among FRC and RC beams with Ø12 rebars and c=70 mm.....	61
Figure 49 P- η results from numerical model: comparison among FRC and RC beams with Ø25 rebars and c=20 mm.....	62
Figure 50 P- η results from numerical model: comparison among FRC and RC beams with Ø25 rebars and c=70 mm.....	62
Figure 51 Close-up of Figure 47 in serviceability region	64
Figure 52 Close-up of Figure 48 in serviceability region	64
Figure 53 Close-up of Figure 49 in serviceability region	65
Figure 54 Close-up of Figure 50 in serviceability region	65
Figure 55 % tensile reinforcement with respect to % load increment for $\eta_{LIM,1}$	66
Figure 56% tensile reinforcement with respect to % load increment for $\eta_{LIM,2}$	67
Figure 57 M- μ for 12-20-0.5% beam.....	81
Figure 58 M- μ for 12-20-1.0% beam.....	81
Figure 59 M- μ for 12-70-0.5% beam.....	82

Figure 60 M- μ for 12-70-1.0% beam.....	82
Figure 61 M- μ for 25-20-0.5% beam.....	83
Figure 62 M- μ for 25-20-1.0% beam.....	83
Figure 63 M- μ for 25-70-0.5% beam.....	84
Figure 64 M- μ for 25-70-1.0% beam.....	84
Figure 65 P- η comparison for 12-20-0.5% beam	85
Figure 66 P- η comparison for 12-20-1.0% beam	85
Figure 67 P- η comparison for 12-70-0.5% beam	86
Figure 68 P- η comparison for 12-70-1.0% beam	86
Figure 69 P- η comparison for 25-20-0.5% beam	87
Figure 70 P- η comparison for 25-20-1.0% beam	87
Figure 71 P- η comparison for 25-70-0.5% beam	88
Figure 72 P- η comparison for 25-70-1.0% beam	88

7 Table index

Table 1 Composition of concrete per m ³ for preliminary tests.....	24
Table 2 Summary of batches and characteristic strength taken by preliminary tests	26
Table 3 Tensile residual strengths of FRCs in preliminary tests [2]	27
Table 4 Results for cylinder compression and indirect tension tests for SCC.....	28
Table 5 Tensile residual strengths according to EN 14651	30
Table 6 Minimum requirement according to MC2010	30
Table 7 Estimated ultimate load values	35
Table 8 Constitutive models in European guidelines [22].....	38
Table 9 Characteristics of the constitutive models from guidelines [22]	39
Table 10 Stress-strain equations according to MC2010	43
Table 11 Estimated mean strength values of FRC beams	46
Table 12 Equivalent flexural stresses	48
Table 13 FRC mechanical parameters according to Rilem [11].....	48
Table 14 Tensile strengths according to Rilem [11].....	49
Table 15 Load-Deflection from numerical Model of 12-20-ZZ and 12-70-ZZ beams ..	56
Table 16 Load-Deflection from numerical Model of 25-20-ZZ and 25-70-ZZ beams ..	57
Table 17 Load-Deflection from numerical Model of no fibres and no stirrups beams ..	58
Table 18 Load-Deflection from numerical Model of beams with stirrups spacing of 10 cm and no fibres.....	58

Table 19 Load-Deflection from numerical Model of beams with stirrups spacing of 30 cm and no fibres.....	59
Table 20 Comparison of load values of FRC and RC beams for fixed values of the deflection	63
Table 21 % tensile reinforcement with respect to % load increment for $\eta_{LIM,1}$	67
Table 22 % tensile reinforcement with respect to % load increment for $\eta_{LIM,2}$	68

8 Bibliografy

- [1] International Energy Agency (IEA), *Energy Technology Perspectives: scenario and strategies to 2050*, 2010.
- [2] Groli, G., *Crack width control in RC elements with recycled steel fibres and applications to integral structures: theoretical and experimental study*, PhD thesis, Polytechnic University of Madrid, 2014.
- [3] [Online]. Fowler D.W., *Failure, Distress and Repair of Concrete Structures*, 2009. Available: <https://www.sciencedirect.com/topics/materials-science/fiber-reinforced-concrete>.
- [4] Fantilli, A.P., *Calcestruzzo fibro-rinforzato: dalla ricerca alle applicazioni strutturali*, Polytechnic University of Turin, 2019.
- [5] [Online]. Mindess S., *Developments in the Formulation and Reinforcement of Concrete*, 2008. Available: <https://www.sciencedirect.com/topics/materials-science/fiber-reinforced-concrete>.
- [6] [Online]. Furcolo N., *Calcestruzzo fibrorinforzato (FRC), tutto quello che occorre sapere*, 2018. Available: <http://biblus.acca.it/focus/calcestruzzo-fibrorinforzato-frc/>.
- [7] Centoze, G.; Leone, M.; Aiello, M.A., *Reuse of steel fibres from scrap tyres in FRC*. Proceedings of BEFIB 2012, Guimaraes (Portugal), 2012.
- [8] WWF Spain, University of Bath, SPRILUR Group.
- [9] *Norme Tecniche per le Costruzioni*, Consiglio Superiore dei Lavori Pubblici, Italy, 2018.
- [10] *DBV Merkblatt Stahlfaserbeton*, Deutsche Beton Vereins, 2001.

- [11] *RILEM TC 162-TDF. Test and design methods for steel fibre reinforced concrete - σ - ε design method: Final Recommendation*, Mater Struct, 2003.
- [12] *CNR-DT 204. Istruzioni per la Progettazione, l'Esecuzione ed il Controllo di Strutture Fibrorinforzato*, Consiglio Nazionale delle Ricerche, Italia, 2006.
- [13] *UNI EN 14651. Metodo di prova per calcestruzzo con fibre metalliche*, 2007.
- [14] *EHE-08 Instrucción del Hormigón Estructural*, Comisión Permanente del Hormigón (Ministerio de Fomento), 2008.
- [15] *fib Model Code 2010*, Comité Euro-International du Béton-Federation International de la Précontrainte, Paris, 2010.
- [16] Chiaia B; Fantilli A.P.; Vallini P., *Evaluation of crack width in FRC structures and application to tunnel linings*, Mater Struct, 2009.
- [17] Molins C., Arnau O., *Experimental and analytical study of the structural response of segmental tunnel linings based on an in situ loading test. Part 1: Test configuration and execution*, Tunn Undergr Sp Techn, 2011.
- [18] *Linee Guida per la messa in opera del calcestruzzo strutturale*, Servizio Tecnico Centrale del Consiglio Superiore dei Lavori Pubblici, 2017.
- [19] *Linee guida per la valutazione delle caratteristiche del calcestruzzo in opera*, Servizio Tecnico Centrale del Consiglio Superiore dei Lavori Pubblici, 2017.
- [20] *ASTM C1609/1609 M, Standard Test Method for Flexural Performance of Fiber-Reinforced Concrete*, 2012.
- [21] Angelakopoulos, H.; Neocleous, K.; Pilakoutas, K., *Uniaxial compressive behaviour of steel fibre reinforced roller compacted concrete*, Proceeding of fibre content 2011, Prague, 2011.
- [22] Blanca A., Pujadas P., de la Fuente A., Cavalario S., Aguado A., *Application of constitutive models in European codes to RC-FRC*, Universitat Politècnica de Catalunya.
- [23] Tiberti G., Plizzari G.A., Walraven J.C., Blom C.B.M., *Concrete tunnel segments with combined traditional and fiber reinforcement*, London, 2008.

[24] Pérez, A.; Corres, H.; Giraldo, A; Peset, J. Peset. *Cracking of RC members revisited. Influence of cover, f_i/ρ and stirrup spacing. An Experimental and Theoretical Study.* Structural Concrete, 2013.

[25] *Eurocode 2: Design of concrete structures. Part 1-1: General rules and rules for building*, 2004.

9 Annexes

9.1 Moment-Curvature diagrams

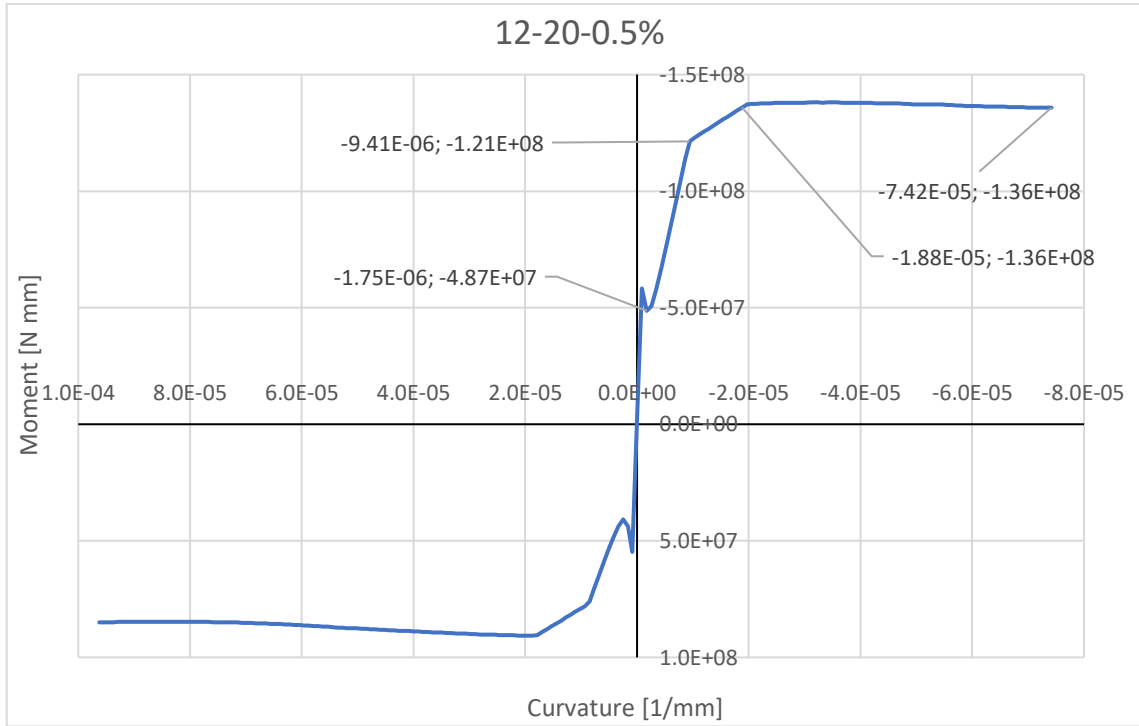


Figure 57 $M-\mu$ for 12-20-0.5% beam

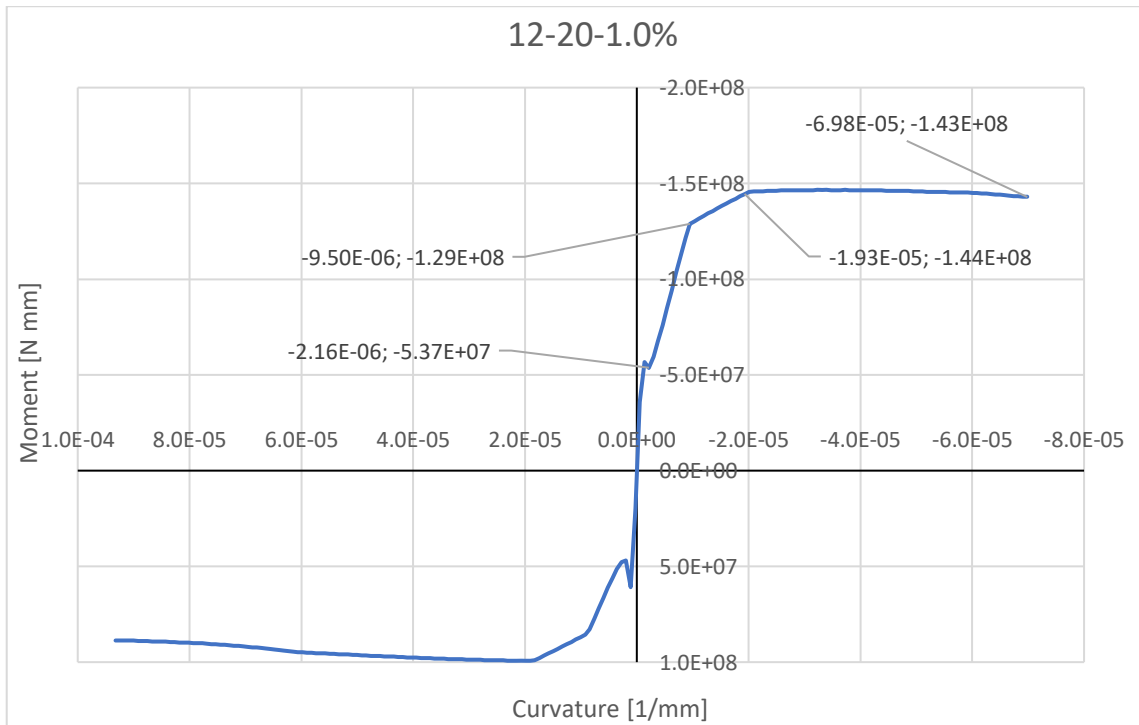


Figure 58 $M-\mu$ for 12-20-1.0% beam

The effect of recycled steel fibres on the deflection of reinforced concrete beams

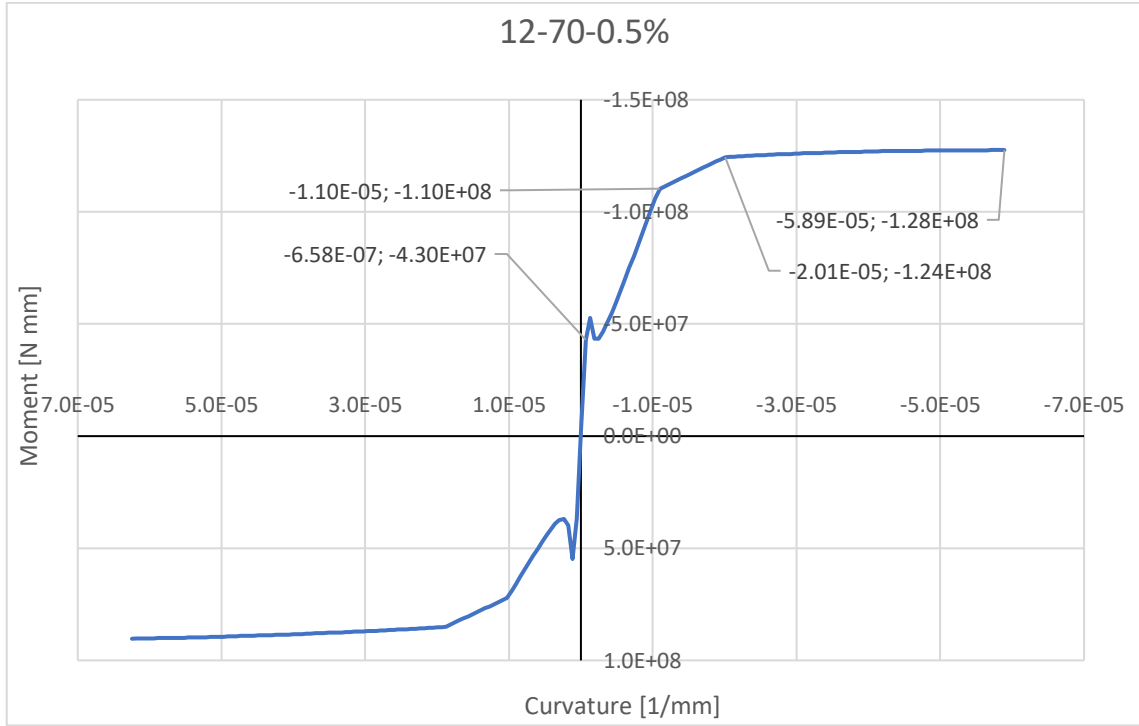


Figure 59 $M-\mu$ for 12-70-0.5% beam

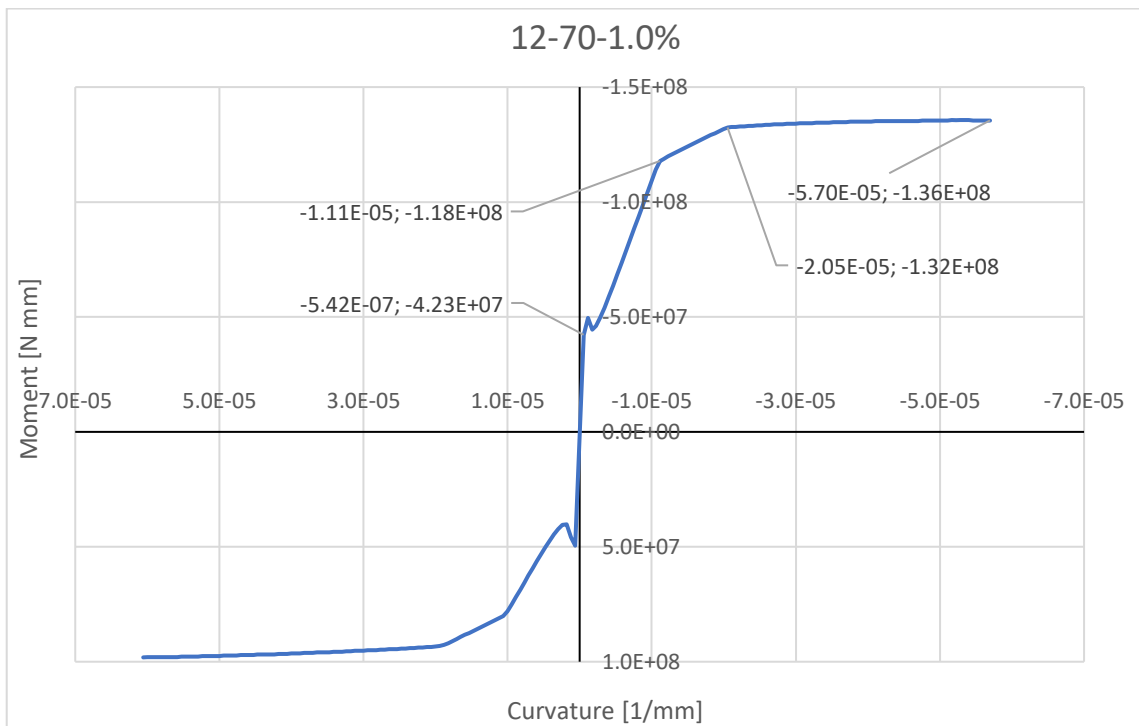


Figure 60 $M-\mu$ for 12-70-1.0% beam

The effect of recycled steel fibres on the deflection of reinforced concrete beams

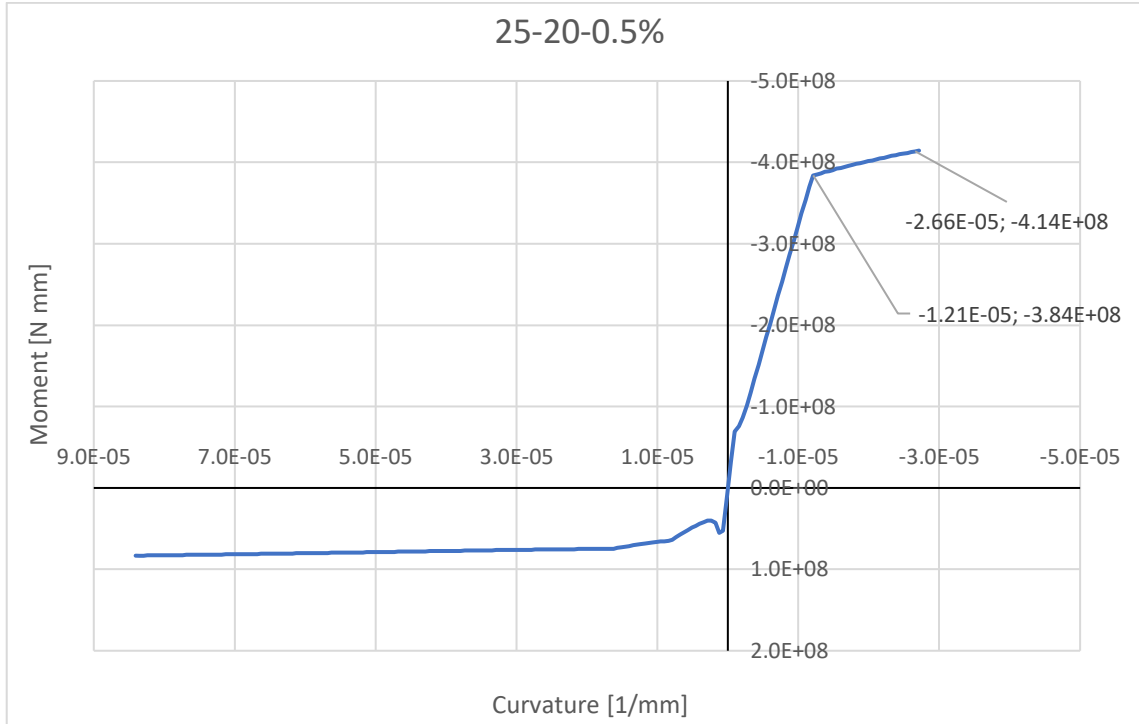


Figure 61 $M-\mu$ for 25-20-0.5% beam

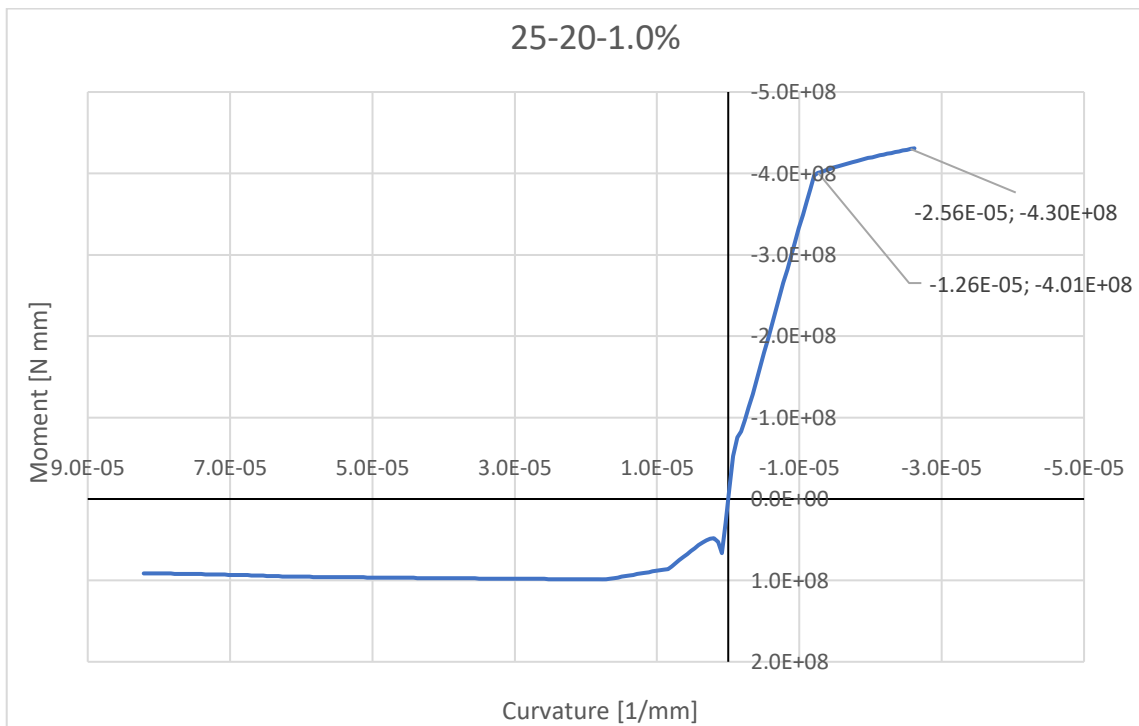


Figure 62 $M-\mu$ for 25-20-1.0% beam

The effect of recycled steel fibres on the deflection of reinforced concrete beams

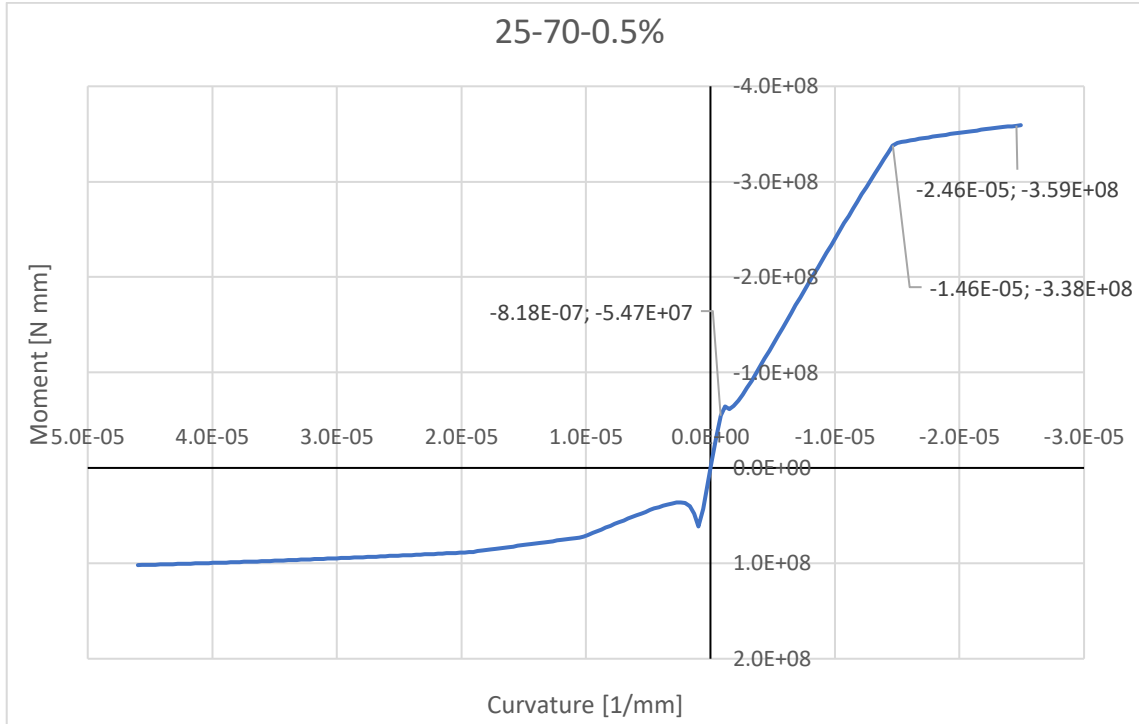


Figure 63 $M-\mu$ for 25-70-0.5% beam

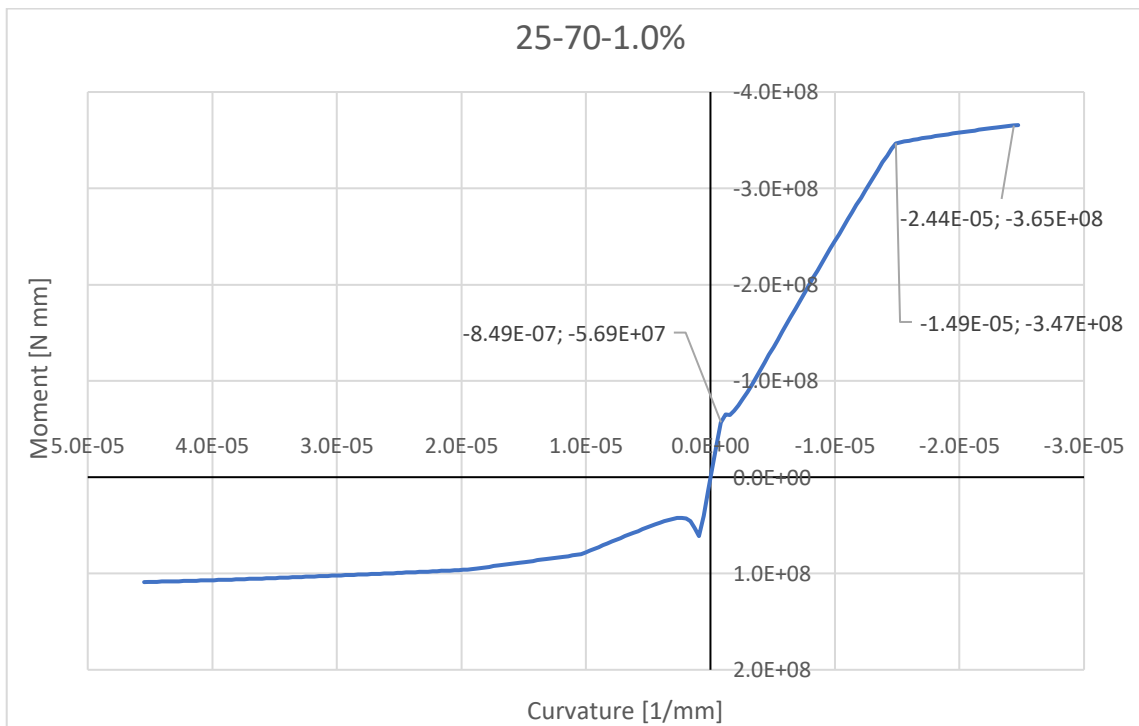


Figure 64 $M-\mu$ for 25-70-1.0% beam

9.2 Comparison between numerical and experimental results

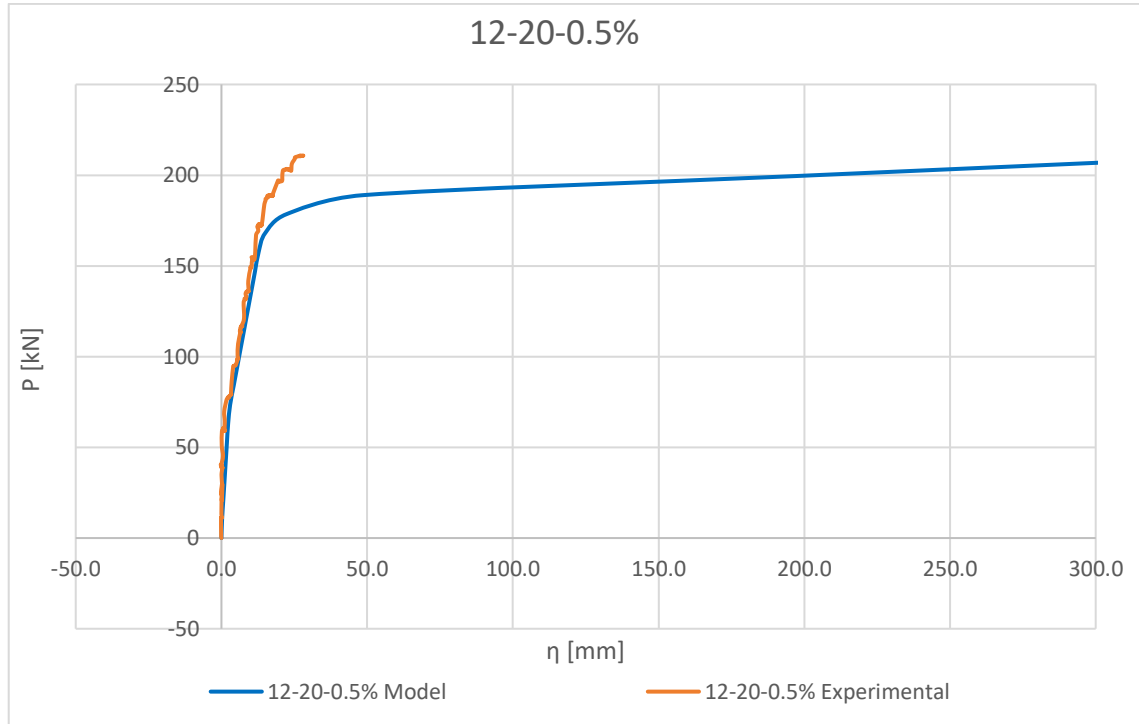


Figure 65 P - η comparison for 12-20-0.5% beam

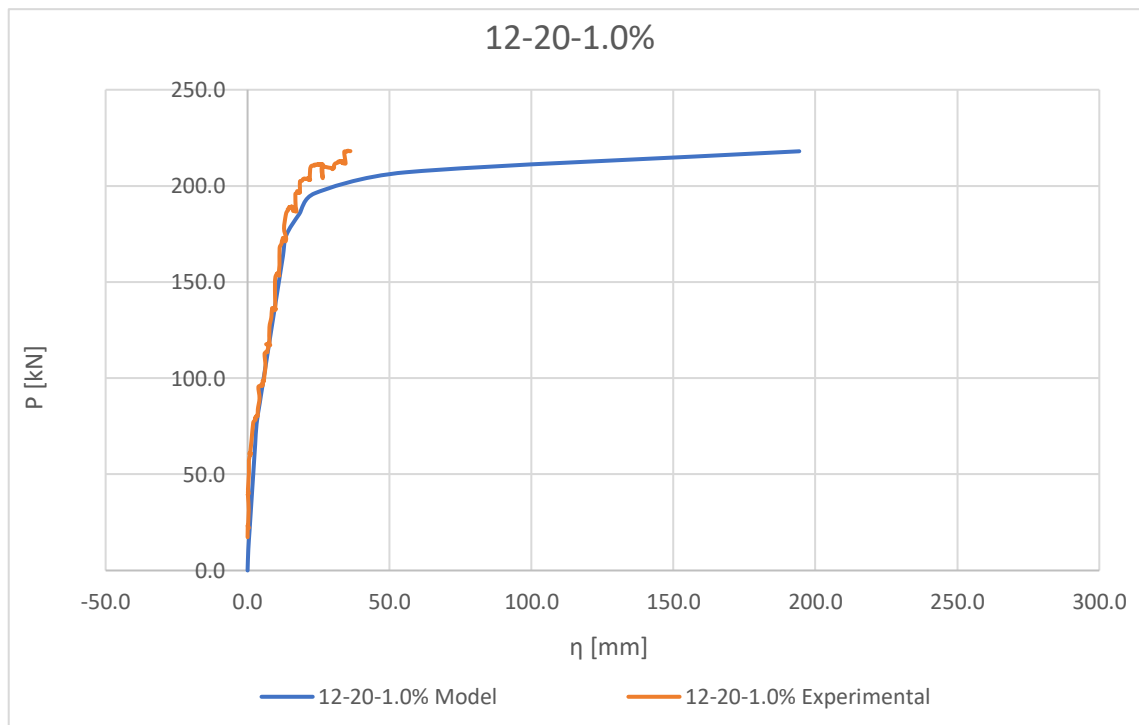


Figure 66 P - η comparison for 12-20-1.0% beam

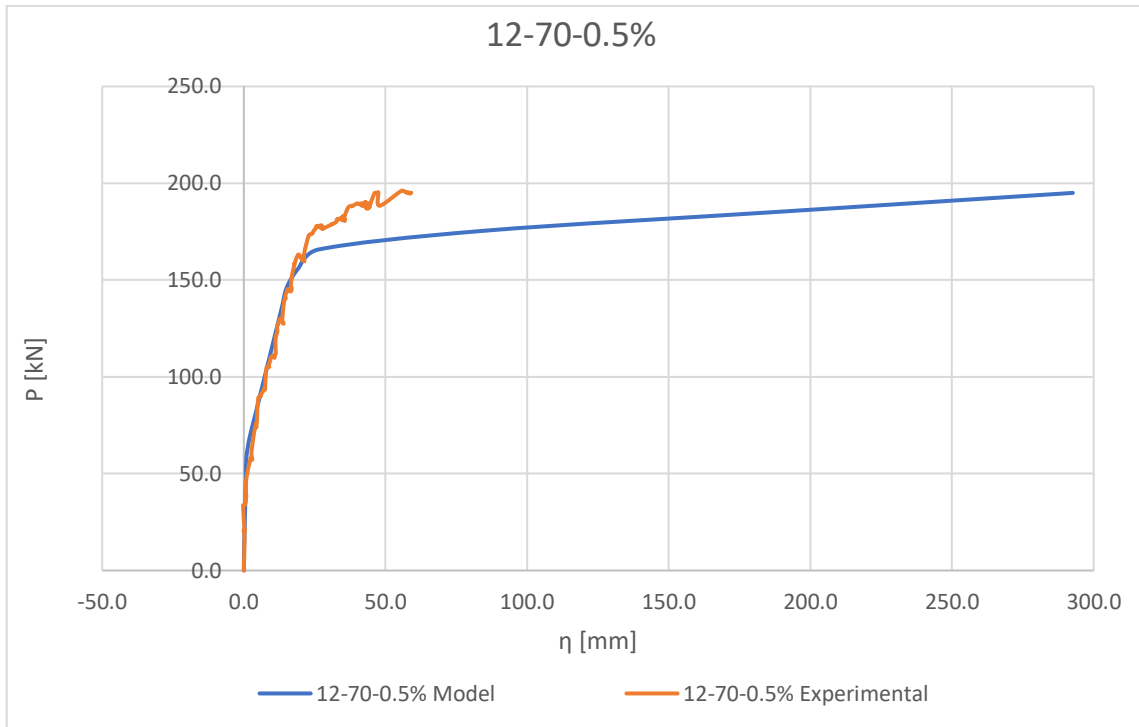


Figure 67 P- η comparison for 12-70-0.5% beam

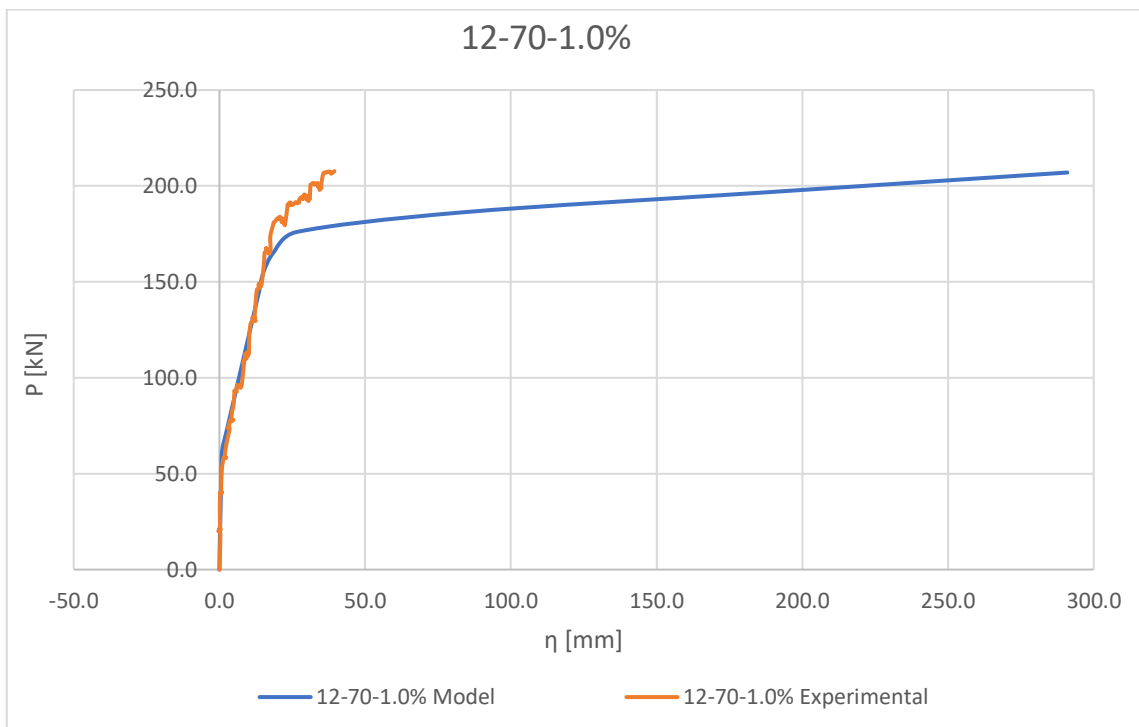


Figure 68 P- η comparison for 12-70-1.0% beam

The effect of recycled steel fibres on the deflection of reinforced concrete beams

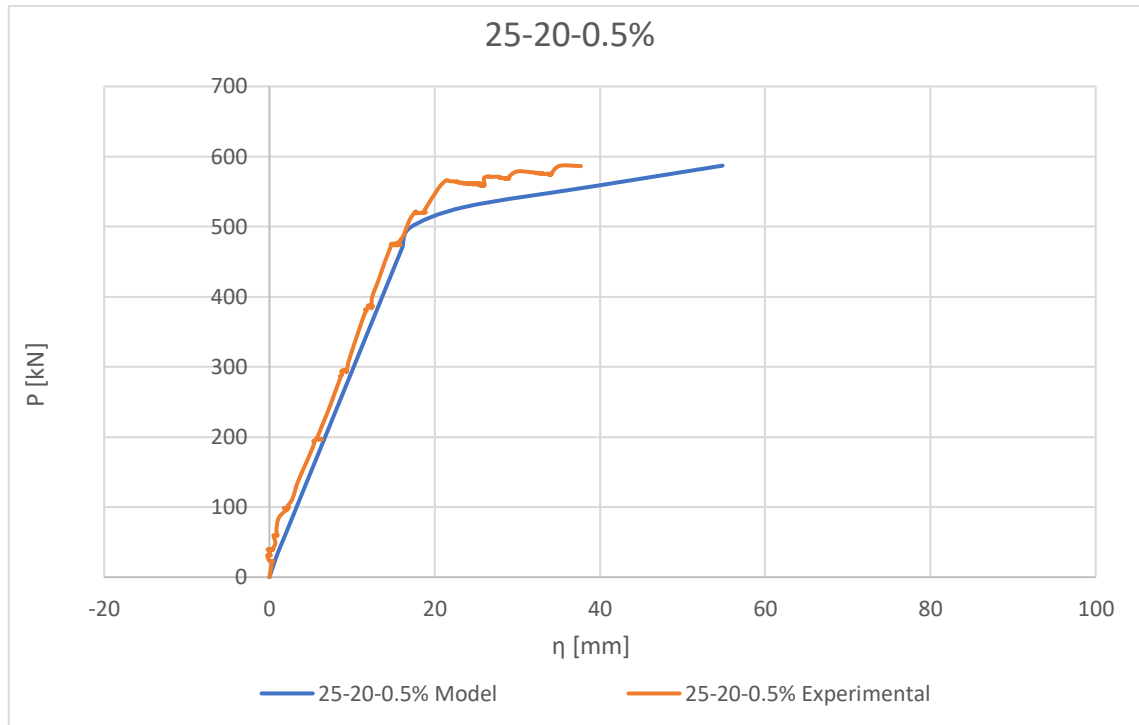


Figure 69 P-η comparison for 25-20-0.5% beam

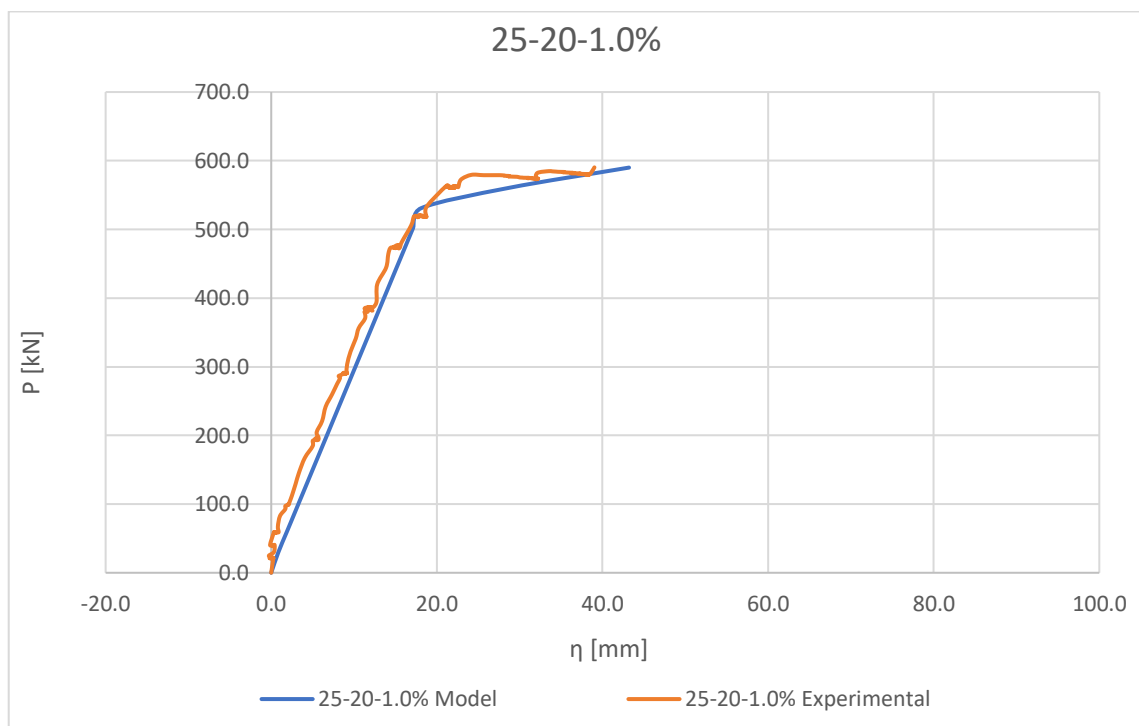


Figure 70 P-η comparison for 25-20-1.0% beam

The effect of recycled steel fibres on the deflection of reinforced concrete beams

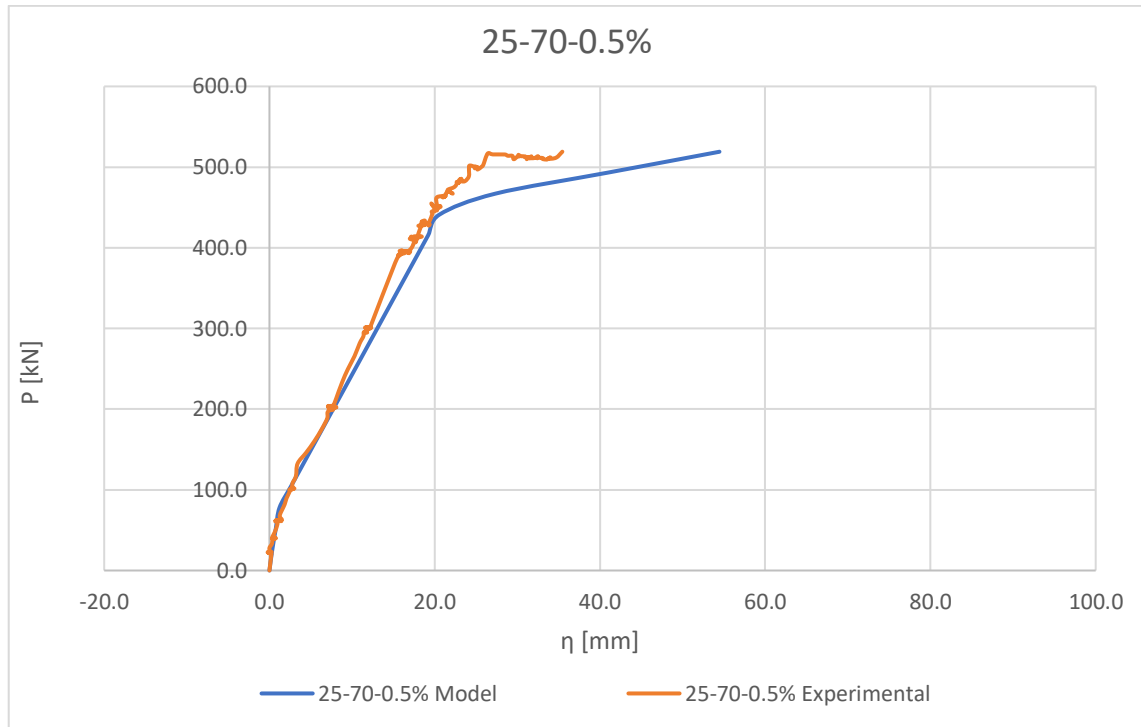


Figure 71 P-η comparison for 25-70-0.5% beam

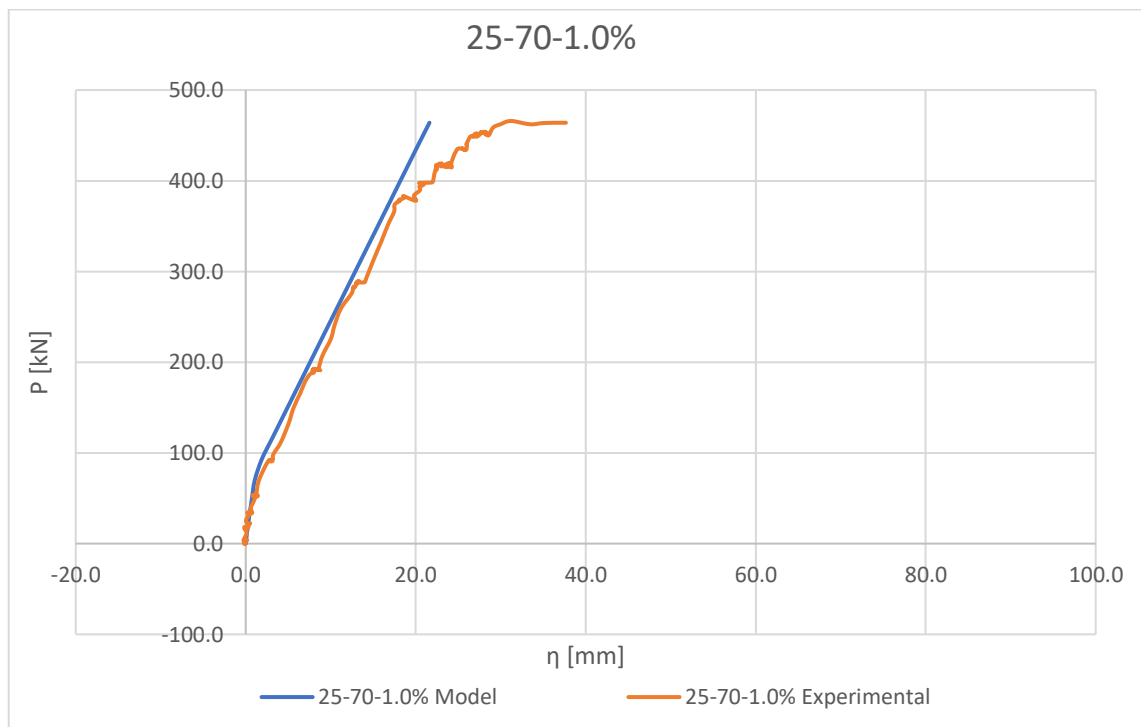


Figure 72 P-η comparison for 25-70-1.0% beam